SIMULATION AND ANALYSIS OF AN ULTRAWIDE-BAND LOG-PERIODIC ANTENNA WITH AN INNOVATIVE STEP-LANE REFLECTOR

Shubhendu Joardar (Guide)
Saptarshi Bose
Bhaswar Chakrabarti
and
Palins Hazra

(Oct.-Nov. 2004)

GMRT Khodad
Tata Institute of Fundamental Research
Narayangaon, Pune-410504

SIMULATION AND ANALYSIS OF AN ULTRAWIDE-BAND LOG-PERIODIC ANTENNA WITH AN INNOVATIVE STEP-LANE REFLECTOR

Shubhendu Joardar
EEngineer-D
(Scientific)

GMRT Khodad
PO-Narayangaon
Dist. Pune - 410504

Saptarshi Bose
Bhaswar Chakrabarti
and
Palins Hazra

Institute of RadioPhysics and Electronics
University of Calcutta

Acknowledgement

We are grateful to our project guide Mr. Shubhendu Joardar for his guidance, involvement and support all along the project. Our special thanks to the director of GMRT, NCRA Professor Rajaram Nityananda for his encouragement during our stay at GMRT. We are indebted to Mr. Sanjay Zinzad (Technical Trainee) for organizing and taking part in the experimental measurements. We would also like to mention the continuous support and encouragement of all the staffs of GMRT.

Saptarshi Bose

Bhaswar Chakrabarti

Palins Hazra

To whomsoever it may concern

I am happy to express that the works carried out in this project has been successful and highly satisfactory to me. The project was difficult to complete due to lack of time but was well accomplished. I wish the students from the Radio Physics and Electronics Dept. of Calcutta university, namely Saptarshi Bose, Bhaswar Chakrabarti and Palins Hazra a bright carrier and successful professional life.

Shubhendu Joardar

Dated : 4-07-2005

CONTENTS

Chapter - I

1. Introduction

1.1 Basic Background

An ideal frequency-independent antenna is physically fixed in size and operates on an instantaneous basis over a wide bandwidth with relatively constant impedance, pattern, polarization and gain [1].

Log-periodic antennas come under the category of frequency independent antennas. The log-periodic structure was first introduced by Raymond DuHamel and Dwight Isbell at the University of Illionis, and in the year 1960 Isbell demonstrated the first log-periodic dipole array [1].

The log-periodic antennas are used in wide band communication in the VHF and UHF range.

Over the years many designs have appeared. Many such designs exist which can be classified under two categories viz. planar structure and dipole structure. The difference in time delay between various frequency signals reaching the antenna plane is of utmost importance for applications in radio astronomy. A flat planar design is preferable for such purposes so as to have a common phase centre for all the frequencies. Such an ultra wide band planar dual polarized log-periodic antenna with an innovative log periodic reflector, which was named as " Step-Lane" reflector was designed and built by our project guide Mr. S.Joardar at the GMRT. This report describes the computer simulation of the same using MATLAB and the experimental results supporting the simulation.

1.2 Objectives

To simulate the structure and the radiation patterns of the antenna mentioned above using MATLAB and experimentally verify the radiation patterns of the antenna at different frequencies.

Chapter – II

2. Frequency Independent Antennas

2.1 Basics

A frequency independent antenna will have impedance and pattern properties that are independent of frequencies. According to Rumsey[1], an antenna will be frequency independent if the shape of the antenna is specified entirely in terms of angles. For example, an infinite logarithmic spiral or a bi-conical antenna with infinite dimensions is a frequency independent antenna. But in case of a finite structure there is reflected wave from the truncation which modifies impedance and pattern characteristics for different frequencies. So, to meet the frequency independent requirement in a finite structure current should be attenuated along the structure and should be negligible at the point of truncation. For radiation and attenuation to occur, charge must be accelerated or decelerated. This happens when a conductor is curved or bent normally along the direction in which the charge is travelling i.e. the structure should be specified in terms of angles [1].

2.2 Fundamentals of Log-Periodic Antennas

One type of antenna configuration, which closely parallels the frequency independent concept, is the log-periodic structure introduced by DuHamel and Isbell[2]. Because the entire shape of it cannot be solely specified by angles, it is not ideally frequency independent. But for certain designs, the amplitude variations are very slight and hence they are practically frequency independent. There are numerous practical structures of the log-periodic antenna, including

log-periodic arrays. In the year 1960, Isbell demonstrated the first log-periodic dipole array(LPDA).

The structure was so called because it repeats periodically with the logarithm of frequency. In other words, the structure doubles for each doubling of the wavelength. The region of high current excitation is known as the active region, and it encompasses 4 to 5 dipole elements. As the frequency changes , the relative voltage and current patterns remain essentially the same, but they move toward the direction of the active region. There is a linear increase in current phase, especially in the active region , from the shorter to the longer elements. This phase shift progression is opposite in direction to that of an unloaded transmission line. It suggests that on the log-periodic antenna structure there is a wave that travels toward the feed forming a unidirectional end fire radiation pattern toward the vertex in the ideal case. The basic concept is that a gradually expanding periodic structure array radiates most effectively when the array elements (dipoles) are near resonance so that with change in frequency the active(radiating) region moves along the array. For higher frequencies, the region containing shorter dipoles is active, and the active region moves to the longer dipoles with decreasing frequency. It is observed that the current concentration is very strong at or near the edges of the conductors of the antenna structure.

The periodicity of the structure does not ensure broadband operation. However, if the variations of the impedance, pattern, directivity, and so forth within one cycle are made sufficiently small and acceptable for the corresponding bandwidth of the cycle, broadband characteristics are ensured within acceptable limits of variation. The total bandwidth is determined by the number of repetitive cycles for the given truncated structure.

The cutoff frequencies of the LPDA can be determined by the electrical lengths of the longest and the shortest elements of the structure. The lower cutoff frequency occurs when the longest element is of the order of half the wavelength. However, the higher cutoff frequency occurs when the shortest element is of the order of half the wavelength only when the active region is very narrow[3].

Chapter – III

3. Highlights of the Log-Periodic Antenna with an Innovative "Step-Lane" Reflector Designed at GMRT

3.1 Design Description

An ultra wideband planar log-periodic antenna feed was designed and developed for the frequency range 200 MHz to 2000 MHz. It was designed in such a manner so as to minimize the relative phase error that develops when the frequency sensitive elements of the antenna have at least some orientation along the main path of the incident electromagnetic wave. But this structure posse's bidirectional radiation pattern, therefore an innovative "Step-Lane" reflecting structure was developed and introduced at the back of the antenna. As a result a considerable increase in the gain was found over the designed range of frequency since the bidirectional radiation pattern now got transformed into a unidirectional one. The principle used over here was reflecting the leakage portion of the incident waves into the planar structure. The reflector was designed in such a way that behind each active region corresponding to a particular band of frequencies in the planar structure, a half wavelength plane reflector was placed. The width of the reflector elements were kept equal to that of the corresponding antenna elements (Fig.1).

The gain of the antenna lies within 9 and 13dBi in both planes of polarization over the entire frequency band.

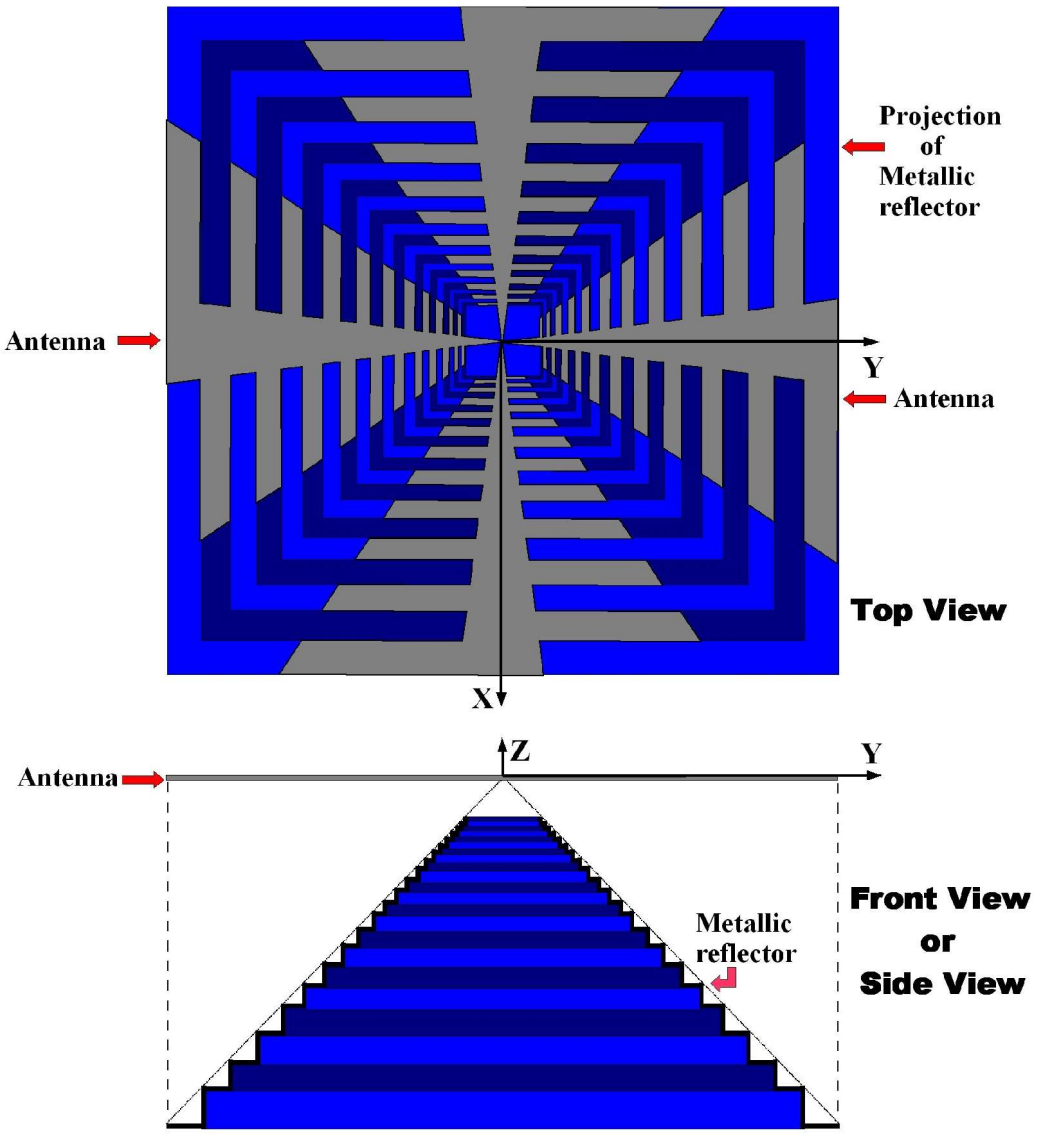

Fig. 1 Front and top views of a planar log-periodic antenna with a log-periodic (Step-Lane) reflector

Chapter – IV

4.Theoretical Analysis of the Log-Periodic Antenna

4.1 Introduction

Theoretical analysis of the antenna has been done with RWG elements using the method of moments in MATLAB.

4.2 Method of Analysis

The method of moments used in the analysis depends on RWG (Rao-Wilton-Glisson) edge elements. First, the surface of a metallic antenna under test is divided into separate triangles as shown in Fig.2a. Each triangle is subdivided into nine sub triangles by using one-third rule. This is done by Delaunay Triangulation algorithm [4]. Two triangles (shaded area in Fig.2a) together form an edge element.

One of the triangles has a plus sign and the other a minus sign. A vector function(or basis function)

$$\mathbf{f}(\mathbf{r}) = \begin{cases} (l/2A^{+})*\rho^{+}(\mathbf{r}), & \mathbf{r} \text{ in } T^{+} \\ (l/2A^{-})*\rho^{-}(\mathbf{r}), & \mathbf{r} \text{ in } T^{-} \\ 0 & \text{otherwise.} \end{cases}$$

is assigned to the edge element. Here, l is the edge length and A^{+} is the area of the triangle T^{+}, similarly for A^{-}. Vectors ρ^{+} and ρ^{-} are as shown in Fig.2b. Vector ρ^{+} connects the free vertex of the plus triangle to the observation point **r**. Similar is the case for ρ^{-} .

After defining the edge elements, the next step is to find the impedance matrix of the electric field integral equation. The surface current density (a vector) of the antenna surface is the sum of the contributions of the above mentioned vector function over all edge elements, with unknown coefficients are found from the moment equations. The moment equations are a linear system of equations with the impedance matrix Z. Basically, the surface current density is given by an expansion into RWG basis vector function over M edge elements.

The basis function of the edge elements approximately corresponds to a small but finite electric dipole of length d(Fig.2b and c). Thus the division of the antenna structure into RWG edge elements approximately corresponds to the division of the antenna current into small elementary electric dipoles (Fig.2a).

In this sense, the impedance matrix Z describes the interaction between different elementary dipoles. The size of the impedance matrix is equal the number of the edge elements. This contribution can be calculated analytically (using the analytical solution for the finite dipole) or by employing the electric field integral equations.

The RWG edge elements are , however more advantageous than simple finite dipoles as shown in Fig.2c. In particular , they support a uniform axial electric current along a thin metal strip[4].

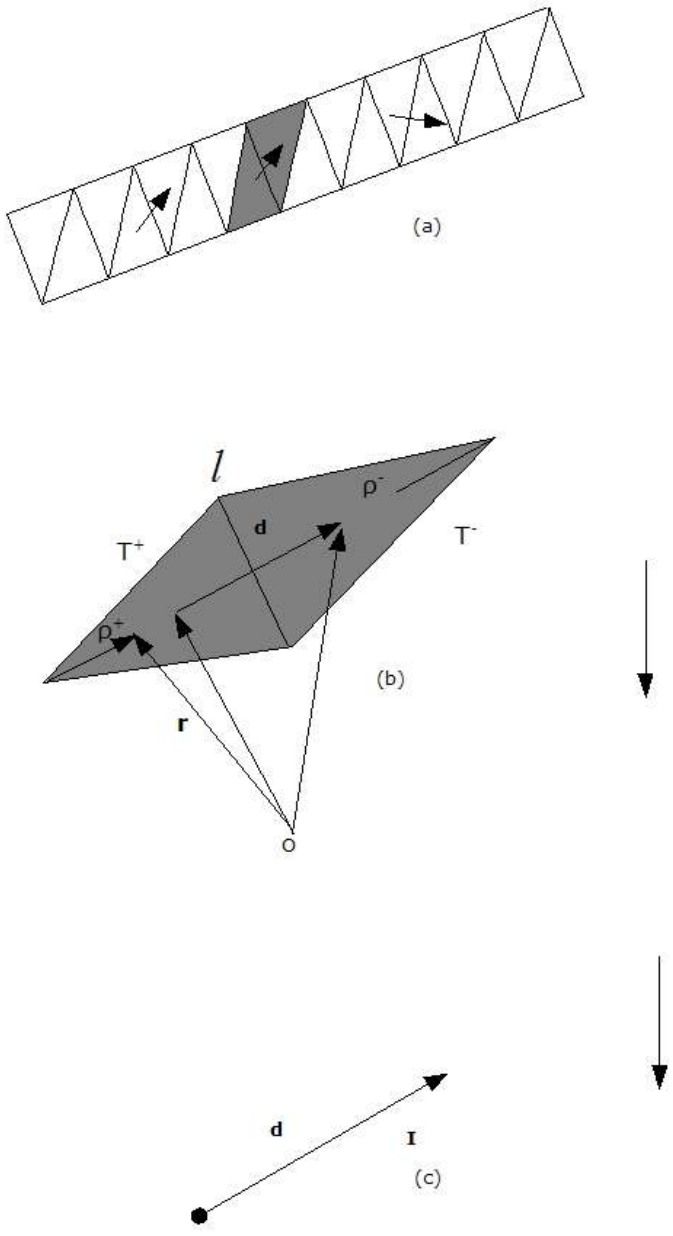

Fig. 2 Schematic of a RWG edge element and the dipole interpretation

4.3 Outline of the Simulation using MATLAB

The log-periodic antenna structure (Fig. 5) was created using the mesh generator of the MATLAB PDE toolbox for generating theoretical radiation patterns and current distributions. The reflector was broken into nearly 400 RWG elements. Instead of a pure log-periodic shape, a simpler model was chosen to avoid complexity. The theoretical analysis was done for a single receiving antenna.

The parameters and associated patterns of the antenna at different frequencies (including the frequencies used by GMRT) which were studied using the simulation with MATLAB are described in the next chapter.

Chapter – V

5.Results and Related Discussions of Theoretical Simulation

5.1 Simulated Structure of the Log-Periodic Feed

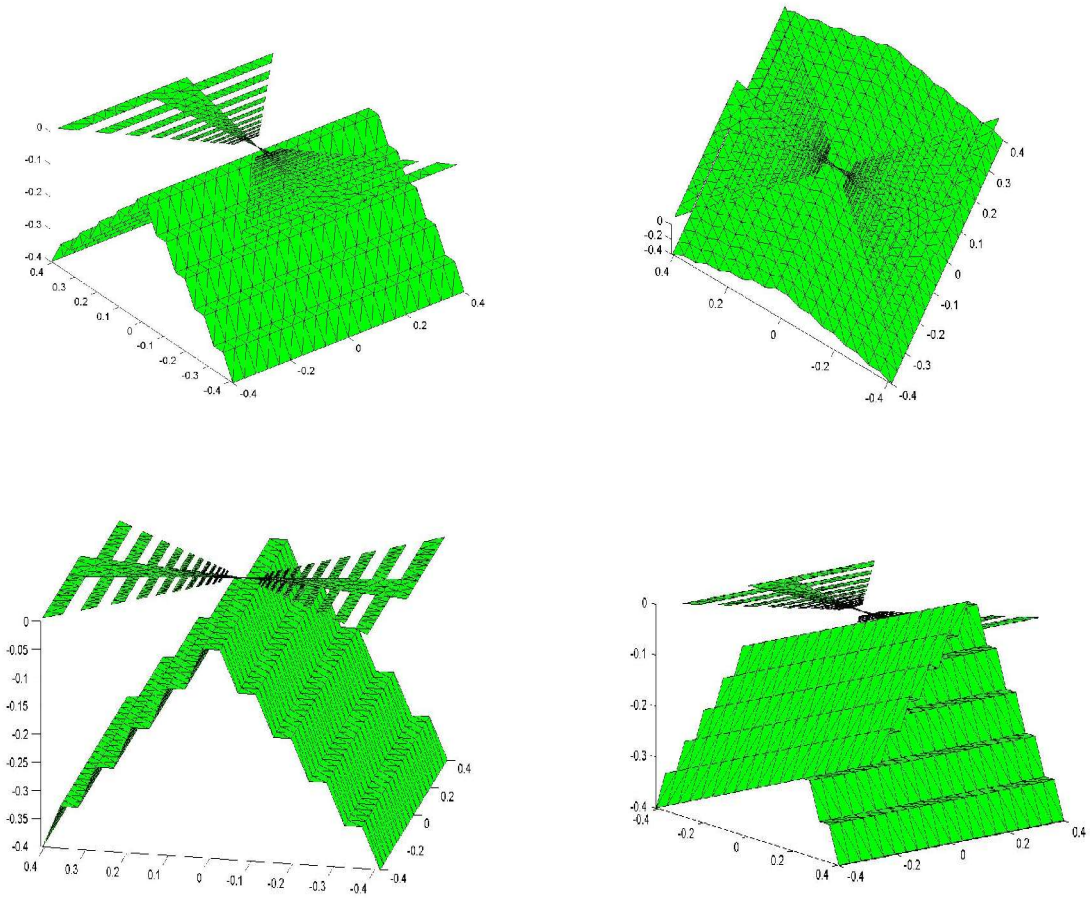

Fig.3 Simulated model of the Log-Periodic antenna feed from various angles (dimensions are in meters)

Fig.3 shows the log-periodic antenna with the innovative step-lane reflector from various viewing angles. The antenna was placed in the x-y plane with the axis of the antenna along y-direction. The figures show how the antenna is mounted symmetrically above the conducting reflector. With changing frequency as different dipoles are activated, corresponding reflecting steps reflect the leakage signal below the antenna surface. As mentioned in the previous chapter, both the antennas and the reflector are created using the mesh generating function of the MATLAB PDE toolbox (refer Appendix – A, for details).

5.2 Parameters and Associated Patterns of the Antenna at Different Frequencies

5.2.1 Current Distribution on the Antenna Surface

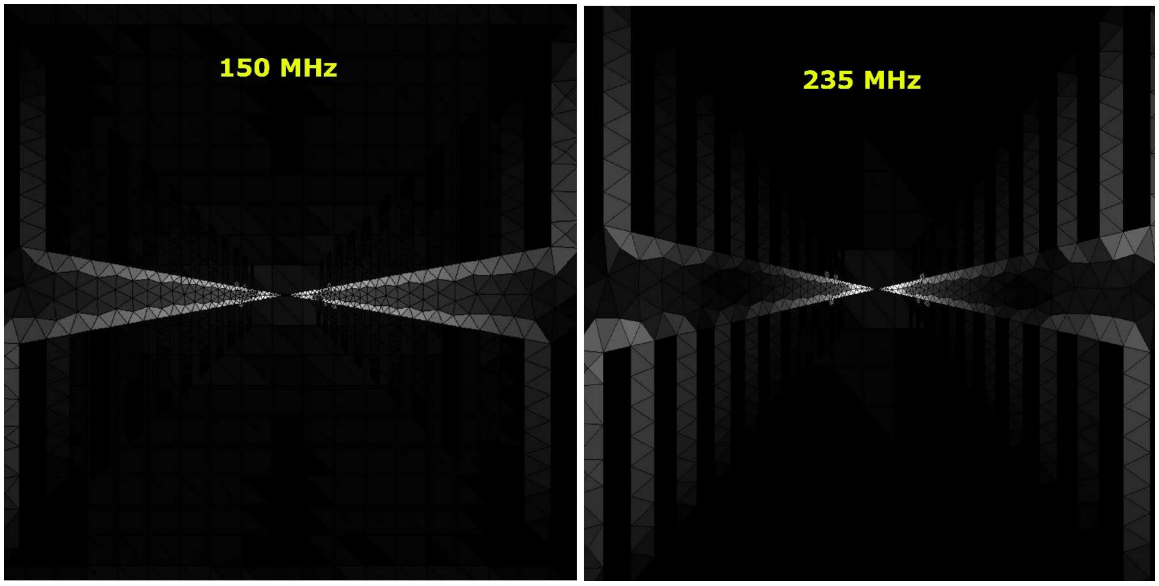

(4-a)★ (4-b)★

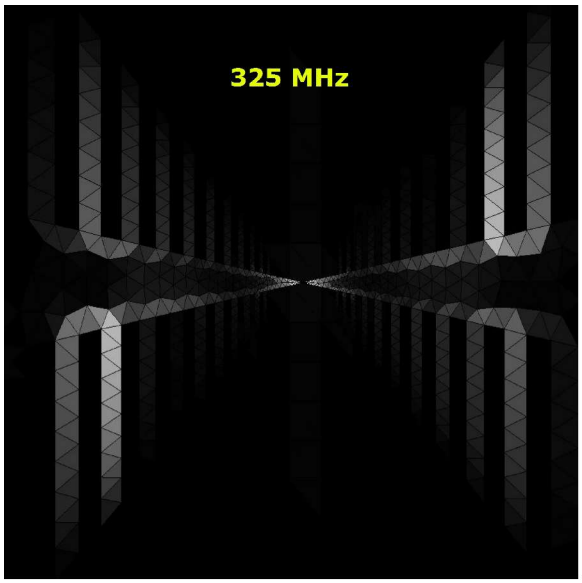

(4-c)

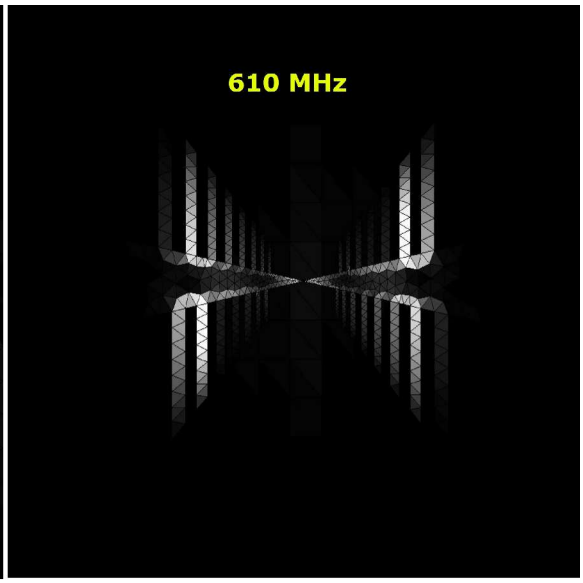

(4-d)

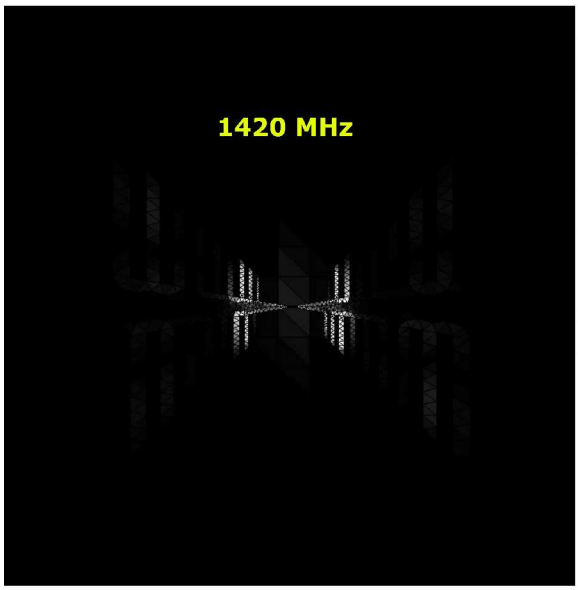

(4-e)

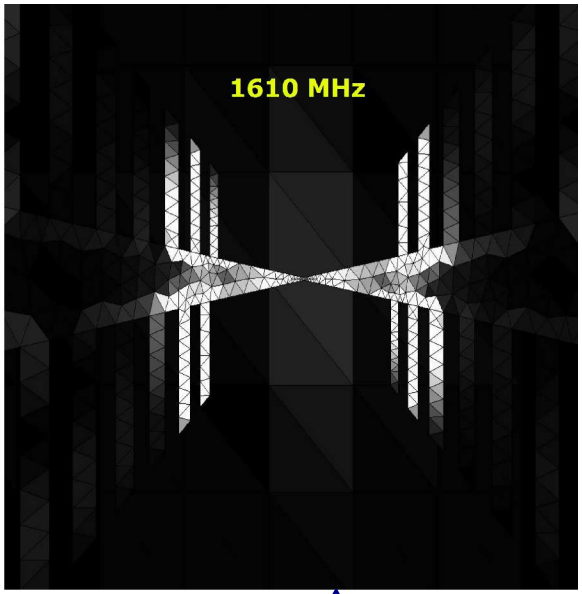

(4-f)

(4-g)

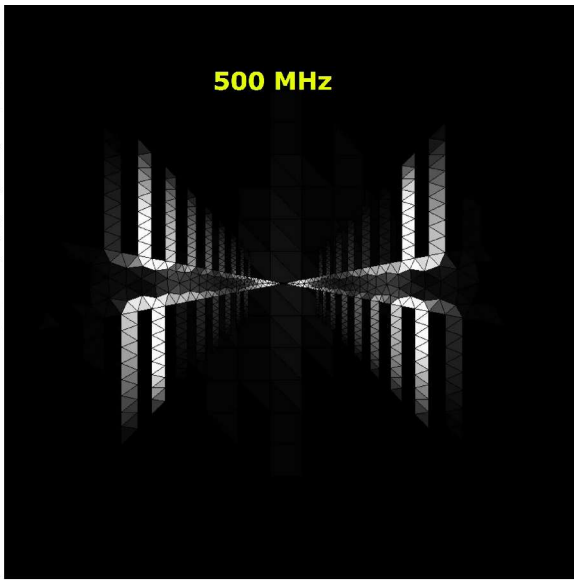

(4-h)

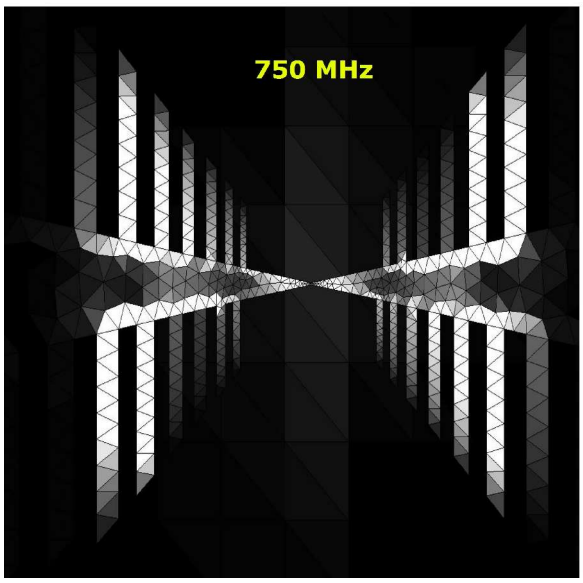

(4-i)

(4-j)

(4-k) (4-l)

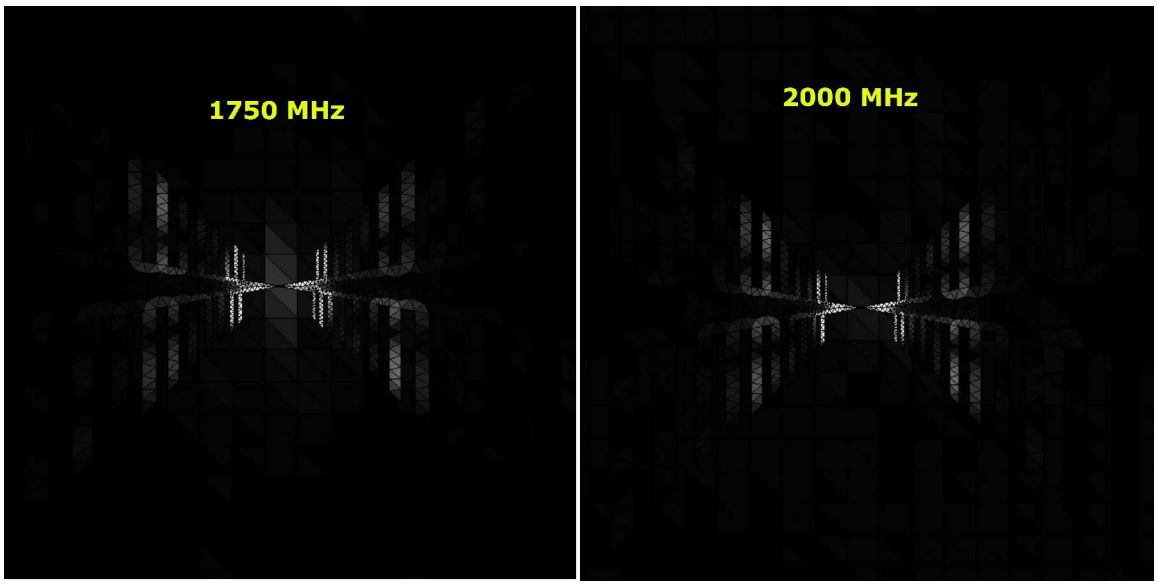

(4-m) (4-n)

Fig.4 Surface current distribution on the antenna

Fig.4 shows the visualization of surface current distribution over the antenna surface. The white colour zones correspond to higher current magnitudes. The more boundary elements we have, the higher the current flow at the edges. The typical structure of the log-periodic antenna meets the above said requirement quite effectively and therefore when the colour bar of the plotting function in MATLAB extends from a minimum to the maximum value of current as in the case of Fig.4 then the current on the rest of the antenna surface appears smaller in comparison with these high values. This is why the middle of the antenna surface looks darker [4]. The major current distribution occurs near the edges of the conductors of the antenna with maximum current density in the active (radiating) region. As is evident from the figure the active region moves from the longer to shorter dipoles as frequency of incident electromagnetic wave increases. This is in agreement with the behavior of surface current density for a practical log-periodic antenna.

N.B. Fig.4-a★ to 4-f★ represent the simulation at GMRT frequencies while Fig.4-g to 4-n represent the simulation for a few other general frequencies.

5.2.2 Surface Current Density along X and Y Direction

In the following Fig.5 (a-n) it is found that the longitudinal component($|\mathbf{J_y}|$) of the current in the direction of the antenna axis dominates the transversal component ($|\mathbf{J_x}|$). The maximum magnitude of the transversal current component is many times smaller than the magnitude of the longitudinal component. It is

also found that that with increasing frequencies the x component of the current shows two small peaks with a hump in between at the centre point.

150 MHz

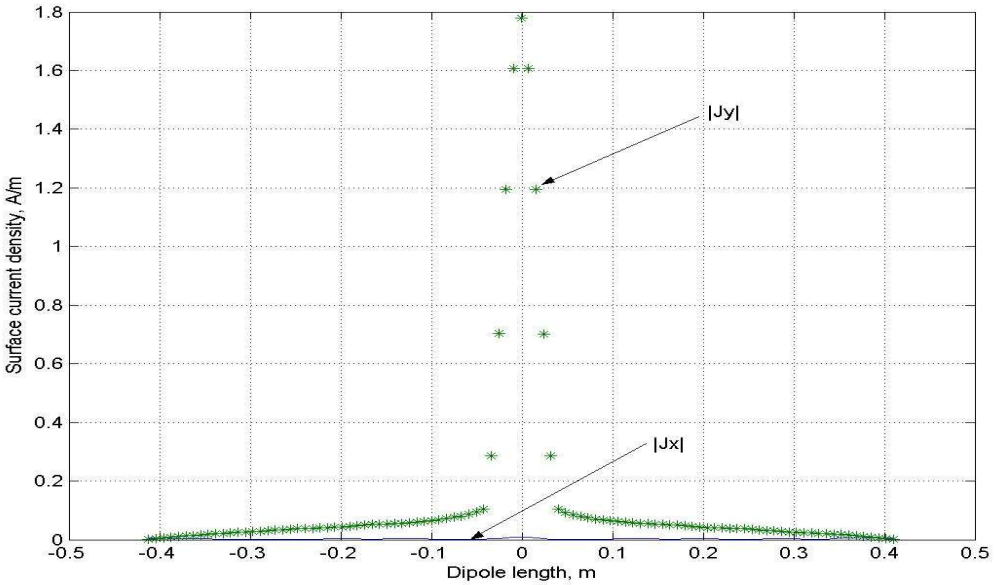

5-a ★

235 MHz

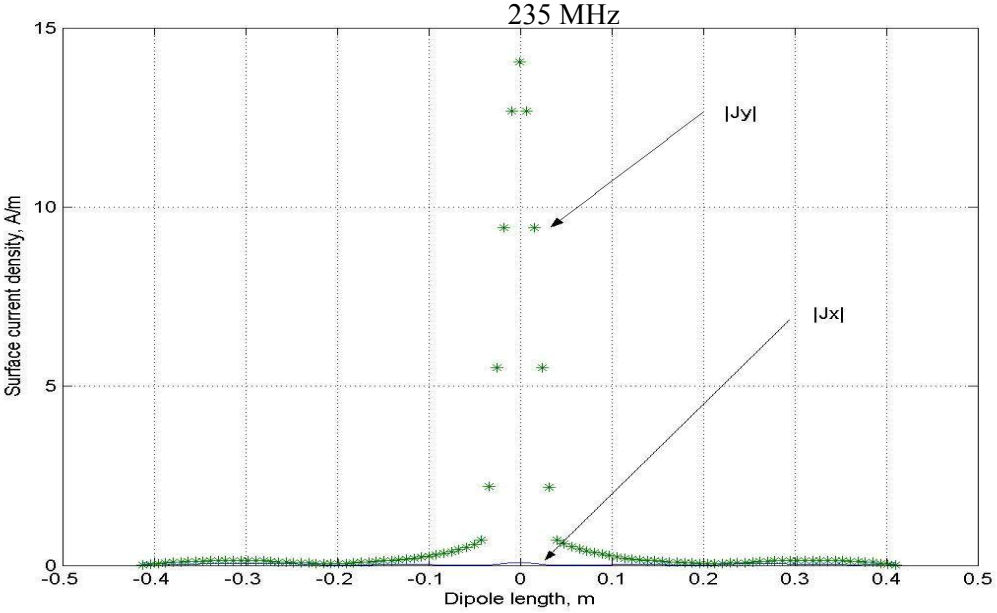

5-b ★

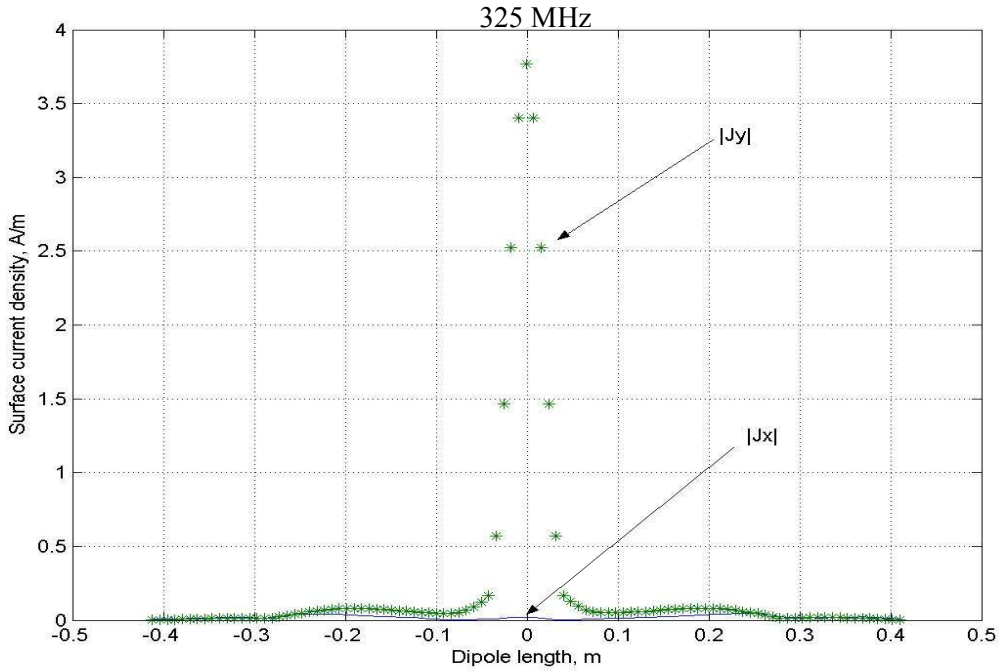
325 MHz
|Jy|
|Jx|
Surface current density, A/m
Dipole length, m

5-c ★

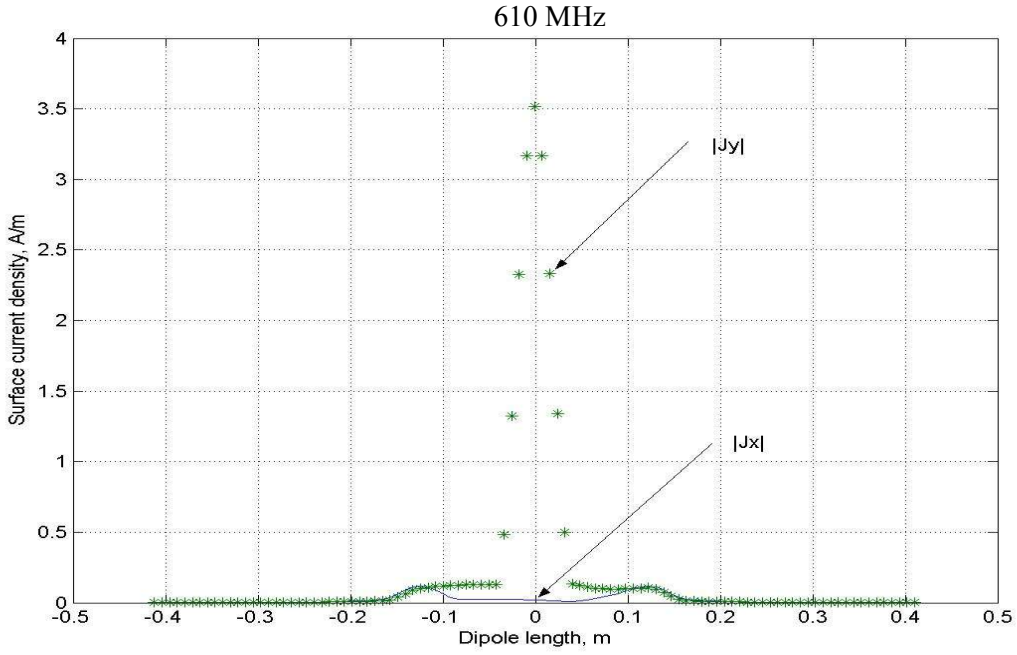
610 MHz
|Jy|
|Jx|
Surface current density, A/m
Dipole length, m

5-d ★

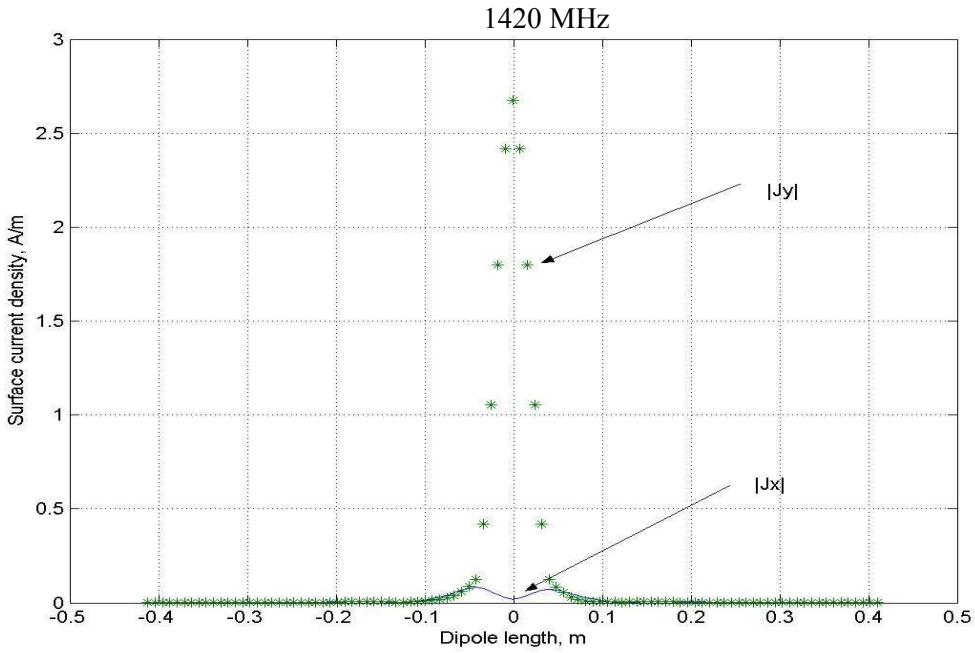
1420 MHz
Surface current density, A/m
Dipole length, m
|Jy|
|Jx|
3
2.5
2
1.5
1
0.5
0
-0.5
-0.4
-0.3
-0.2
-0.1
0
0.1
0.2
0.3
0.4
0.5

5-e ★

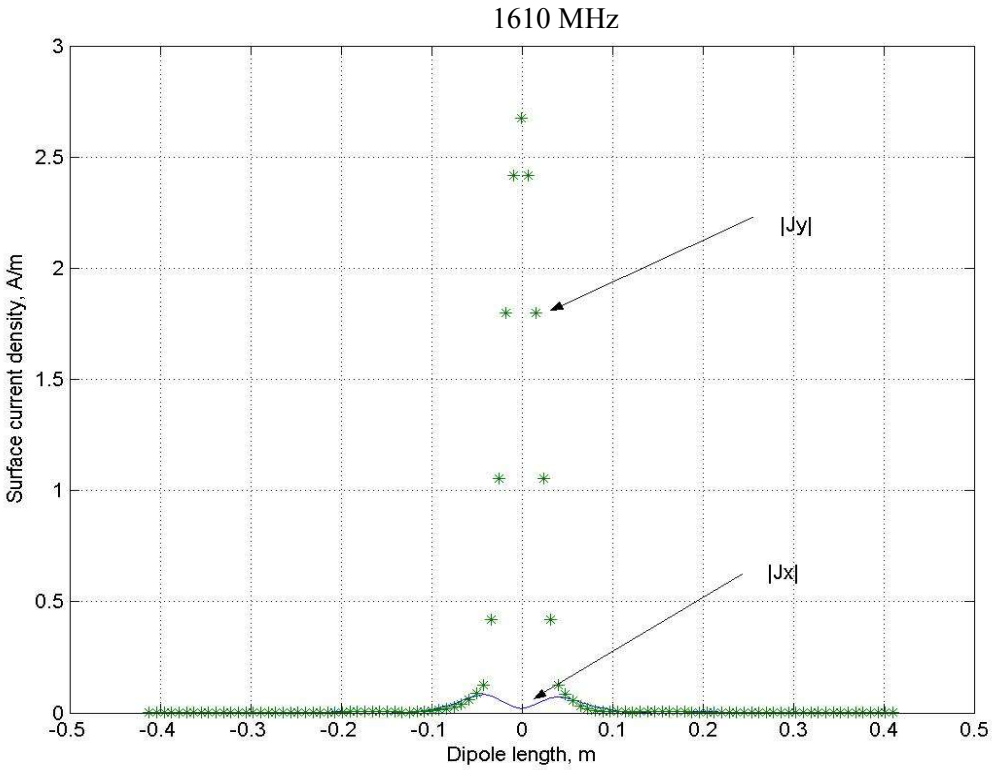
1610 MHz
Surface current density, A/m
Dipole length, m
|Jy|
|Jx|
3
2.5
2
1.5
1
0.5
0
-0.5
-0.4
-0.3
-0.2
-0.1
0
0.1
0.2
0.3
0.4
0.5

5-f ★

250 MHz

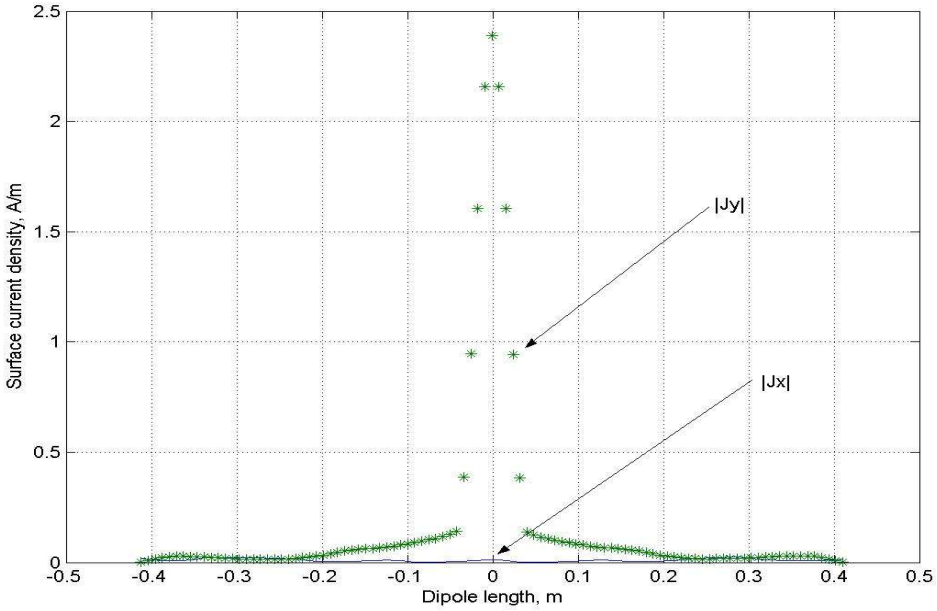

5-g

500 MHz

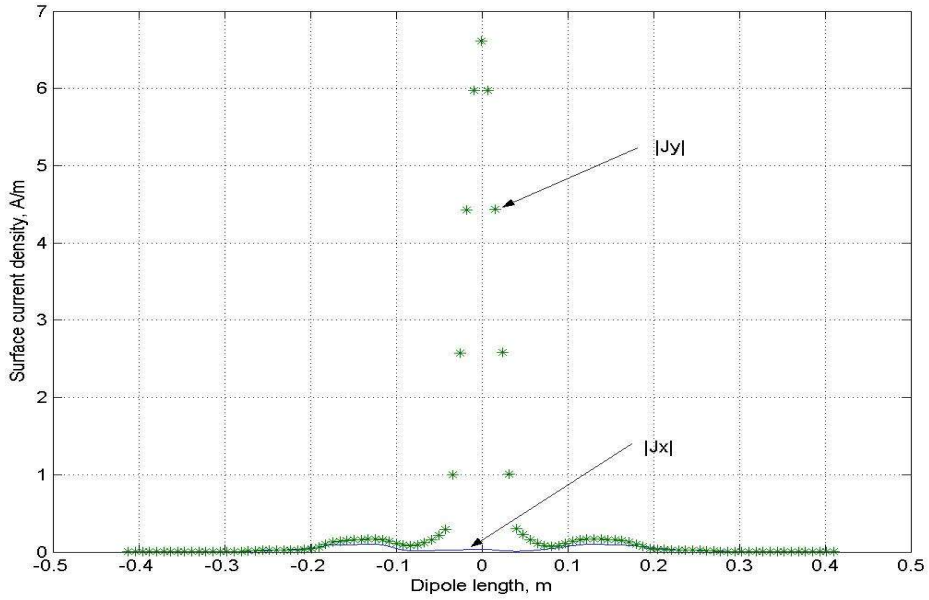

5-h

750 MHz

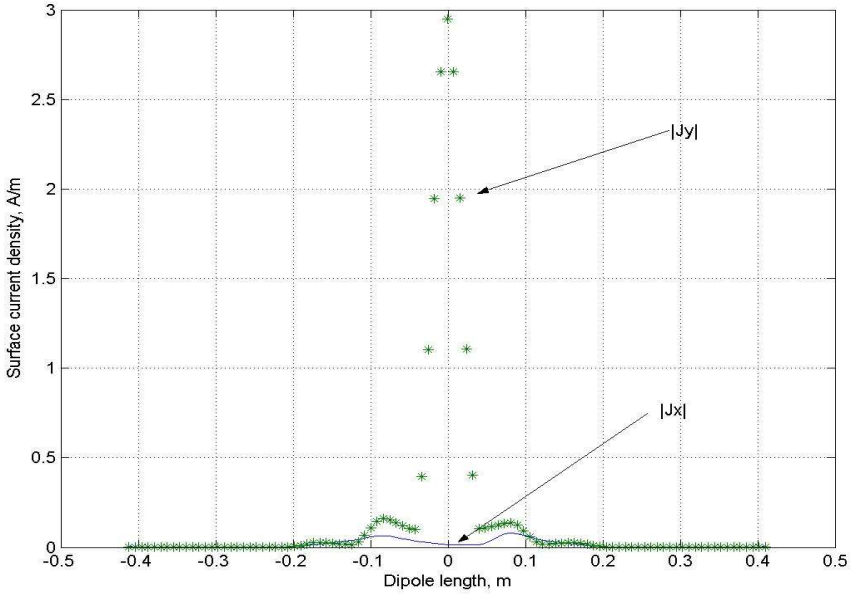

5-i

1000 MHz

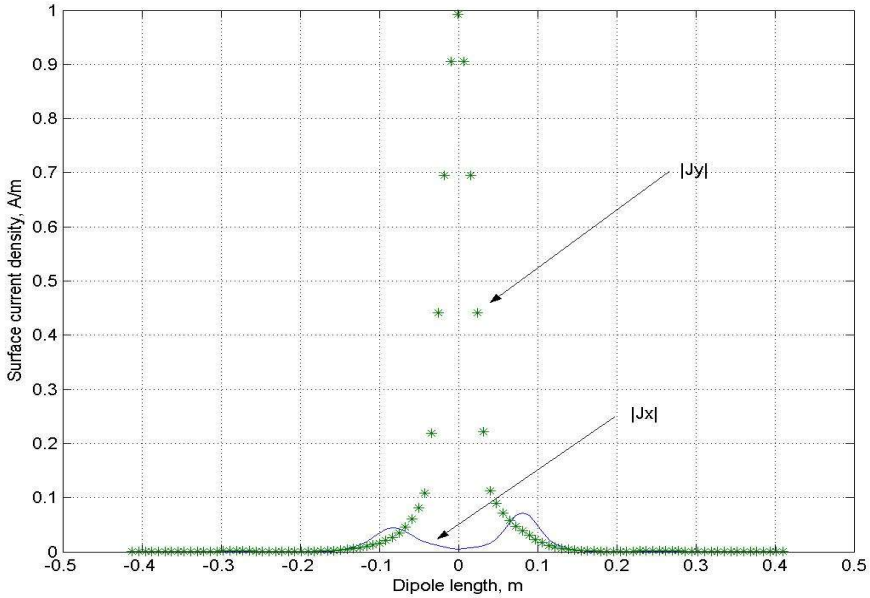

5-j

1250 MHz

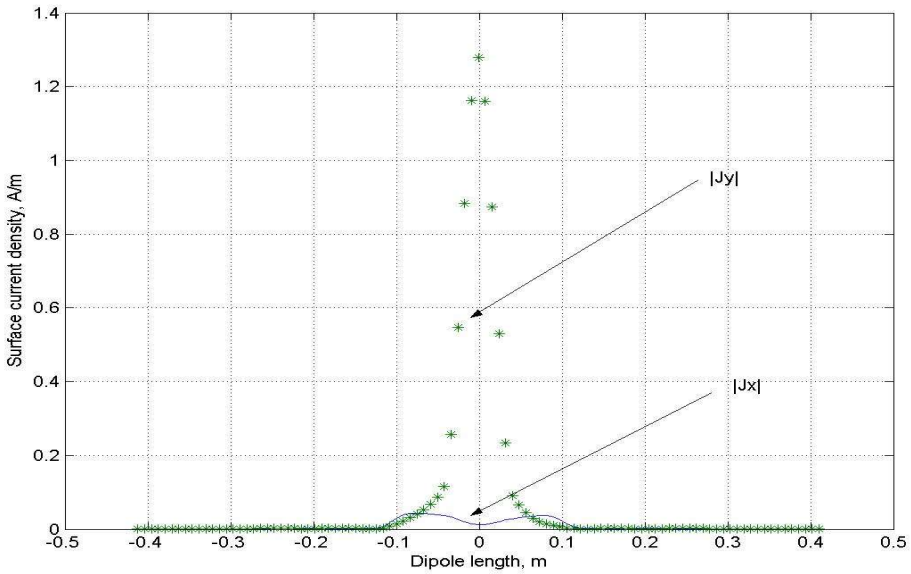

5-k

1500 MHz

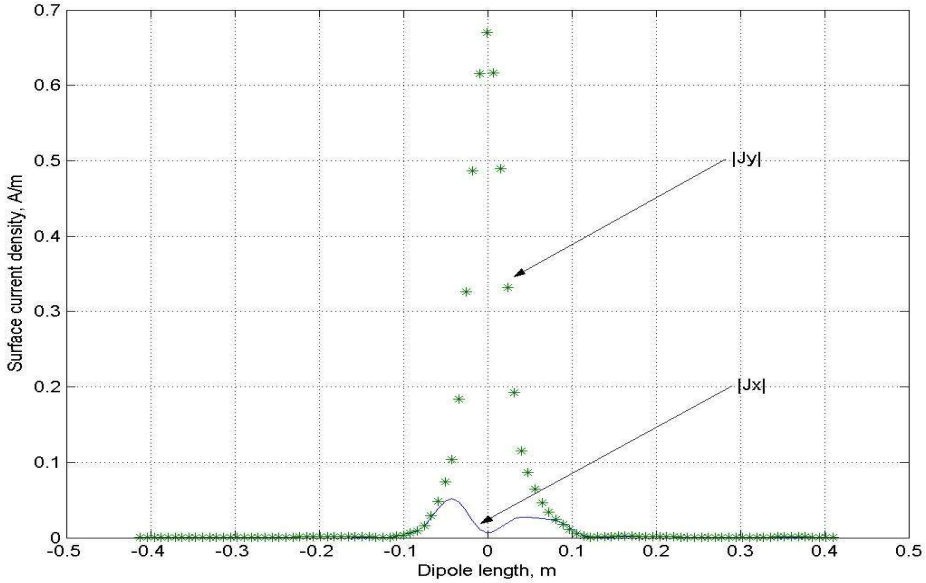

5-l

1750 MHz

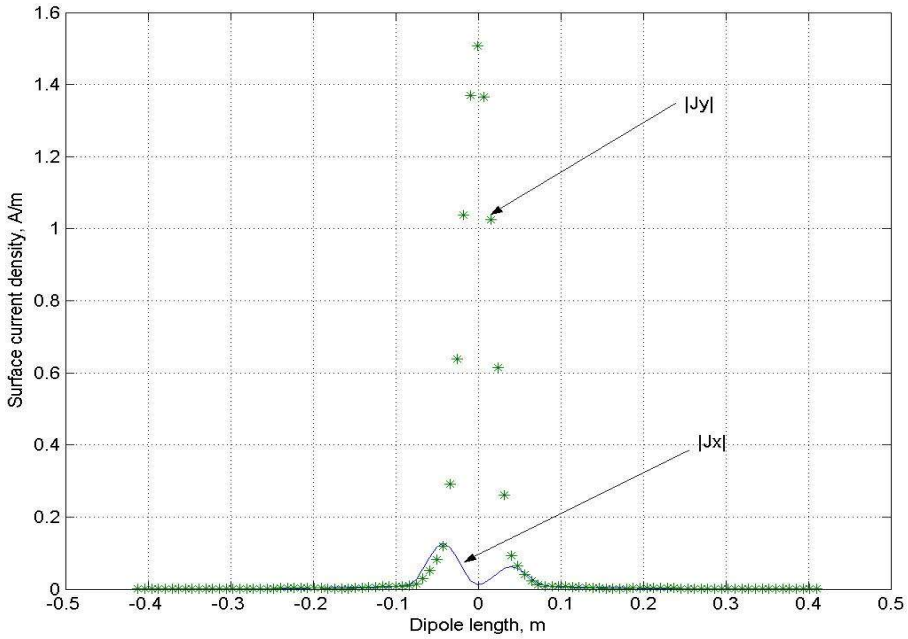

5-m

2000 MHz

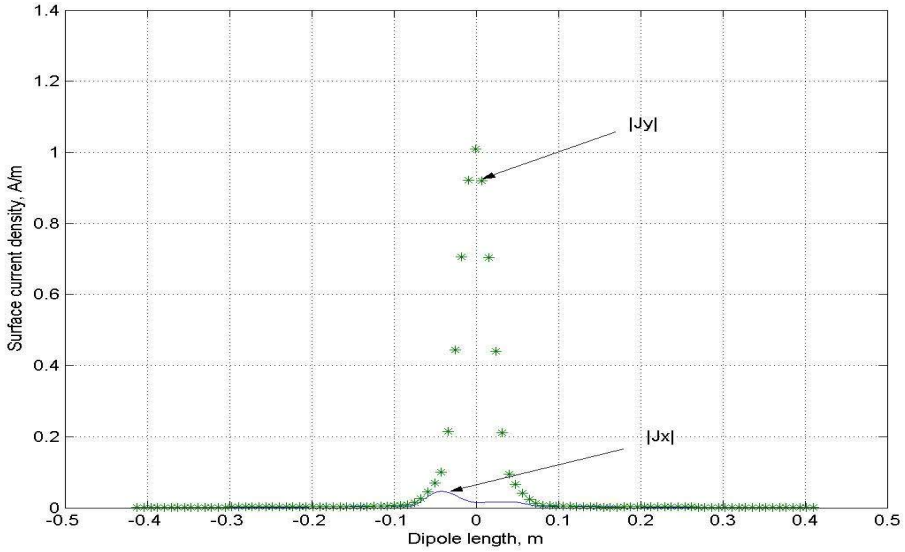

5-n

Fig.5 Surface current density along X and Y direction

In Fig.4 it is seen that for some frequencies the illumination is comparatively poor, than the rest. This can be attributed to smaller values of the longitudinal component of the surface current for those frequencies in Fig.5. Investigation on this observation is on.

N.B. Fig.5-a★ to 5-f ★ represent the simulation at GMRT frequencies while Fig.5-g to 5-n represent the simulation for a few other general frequencies.

5.2.3 Three Dimensional Far Field Pattern of Power, Electric Field and Radiation Intensity

From Fig.(6) it is observed that the generated three dimensional patterns (refer Appendix–B, for details of 3-d plotting algorithm) basically show a bidirectional radiation pattern in broadside way i.e. perpendicular to the paper. Now, as discussed earlier an innovative step-lane reflector was placed behind the antenna to make the pattern unidirectional and make the gain high. It is evident from the figures, that at frequencies below 200 MHz, the radiation pattern is bidirectional with significant back lobes. This is because of the fact that frequencies below 200 MHz are outside the minimum frequency of the designed frequency range of the antenna. With this modelling, at higher frequencies (above 1500 MHz) the back lobes are significant. There is a scope of further improvement in the theoretical model.

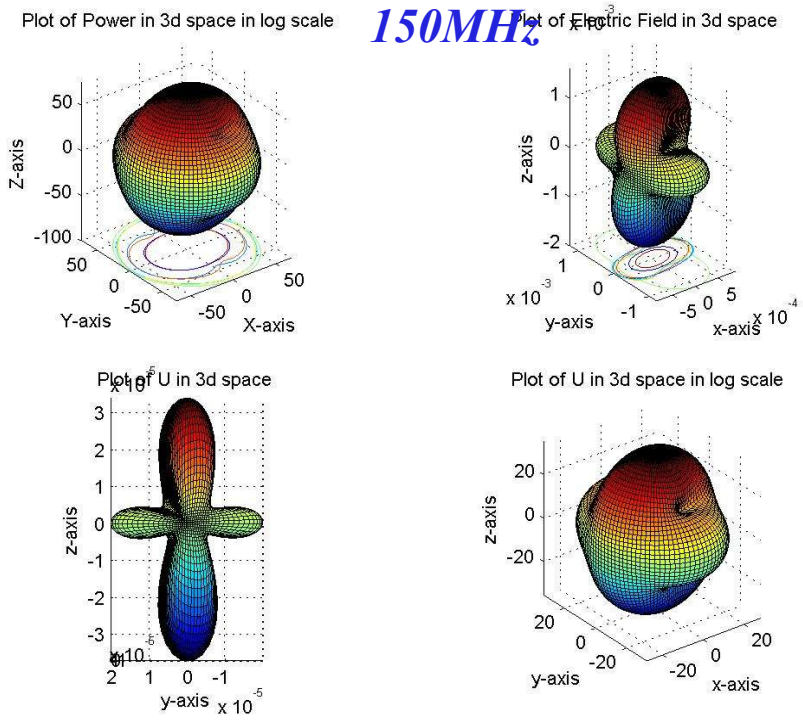

6-a ★

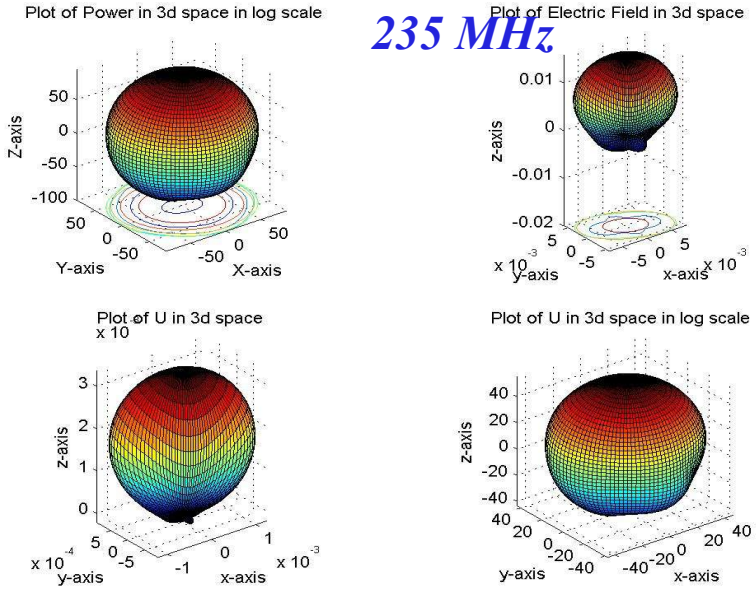
Plot of Power in 3d space in log scale
235 MHz
Plot of Electric Field in 3d space
Z-axis
Y-axis
X-axis
z-axis
y-axis
x-axis
Plot of U in 3d space
Plot of U in 3d space in log scale

6-b ★

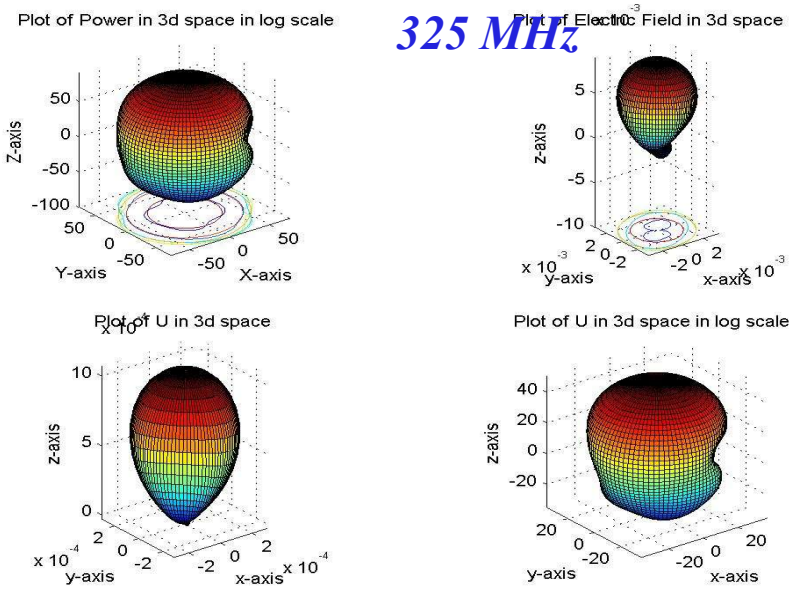
Plot of Power in 3d space in log scale
325 MHz
Plot of Electric Field in 3d space
Z-axis
Y-axis
X-axis
z-axis
y-axis
x-axis
Plot of U in 3d space
Plot of U in 3d space in log scale

6-c ★

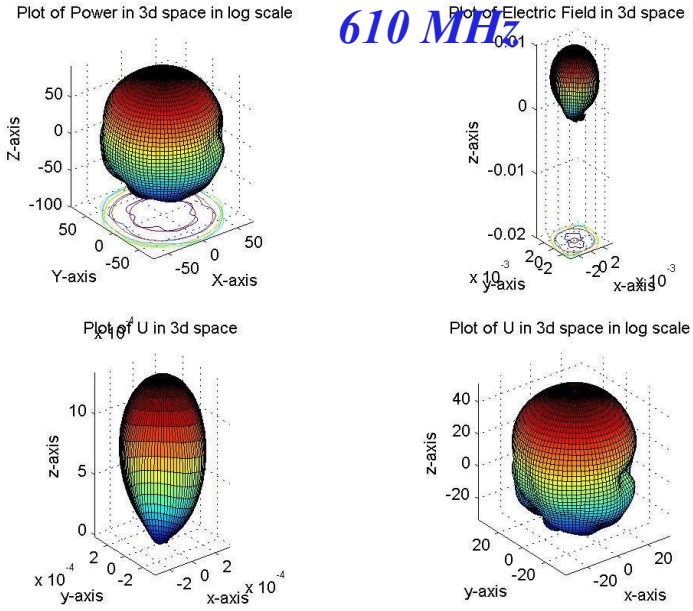
Plot of Power in 3d space in log scale
610 MHz
Plot of Electric Field in 3d space
Z-axis
Y-axis
X-axis
z-axis
y-axis
x-axis
Plot of U in 3d space
Plot of U in 3d space in log scale

6-d ★

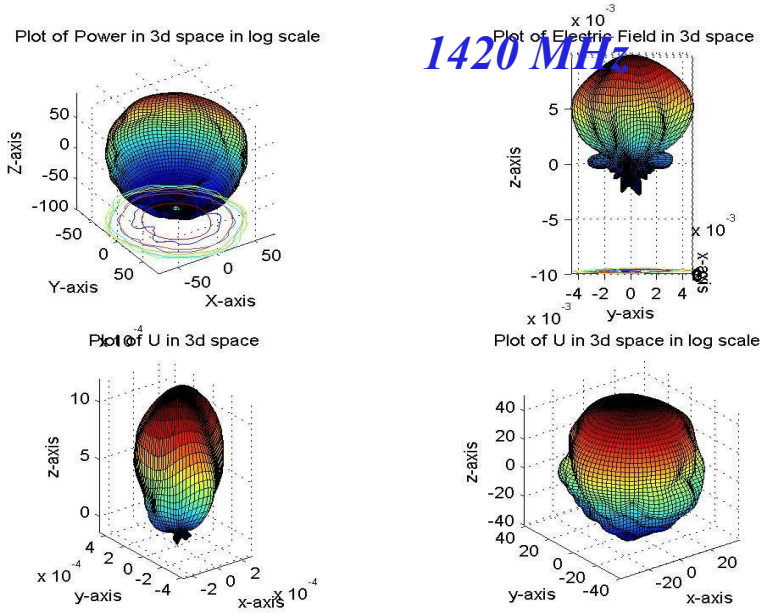
Plot of Power in 3d space in log scale
1420 MHz
Plot of Electric Field in 3d space
Z-axis
Y-axis
X-axis
z-axis
y-axis
x-axis
Plot of U in 3d space
Plot of U in 3d space in log scale

6-e ★

1610 MHz

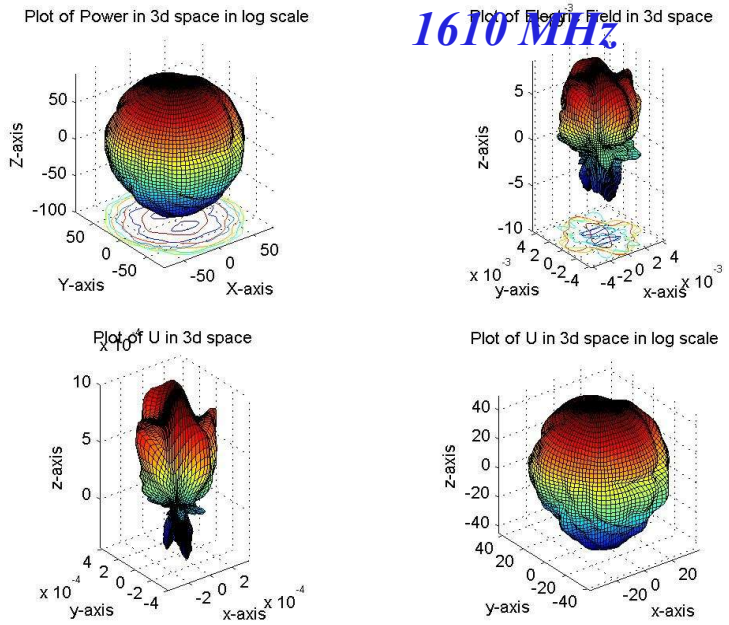

6-f ★

250 MHz

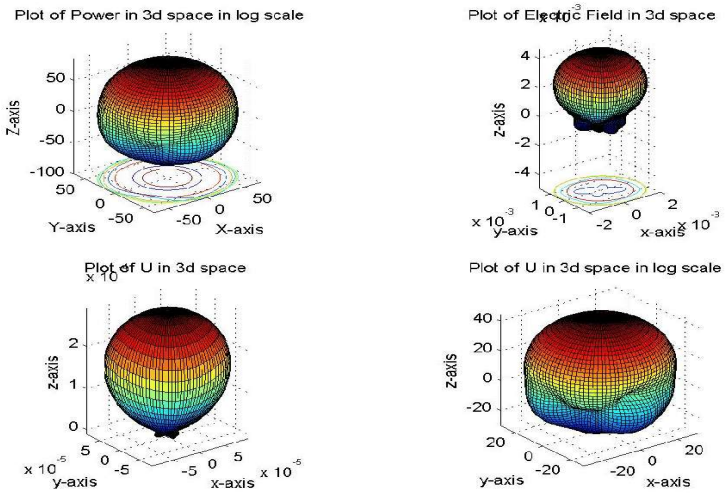

6-g

500 MHz

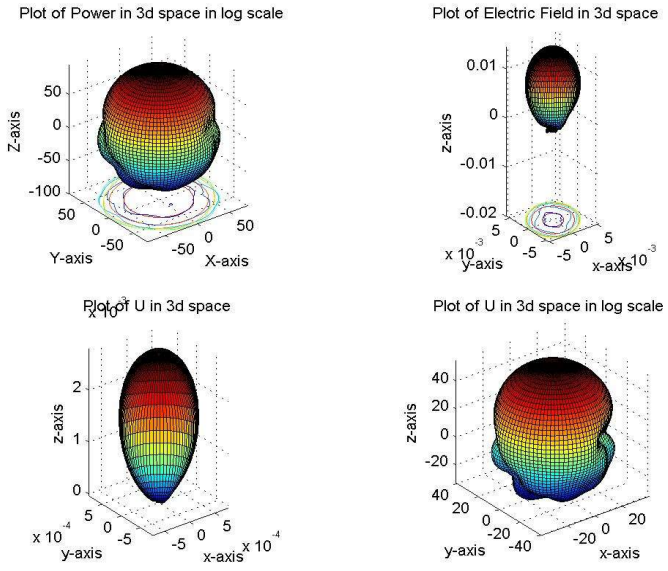

6-h

750 MHz

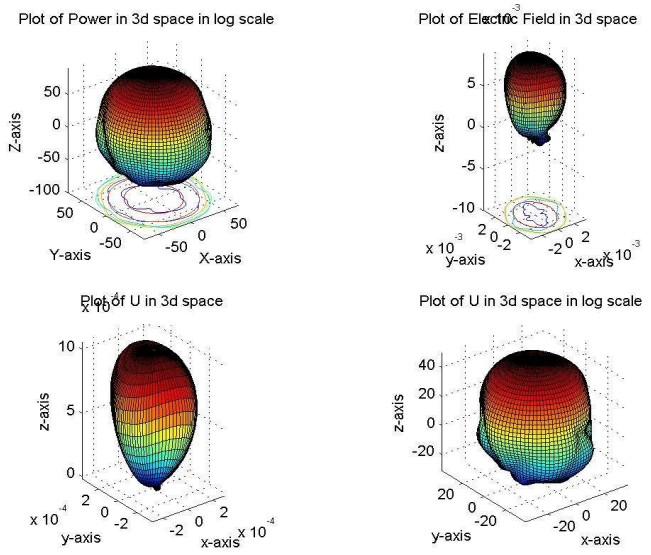

6-i

1000 MHz

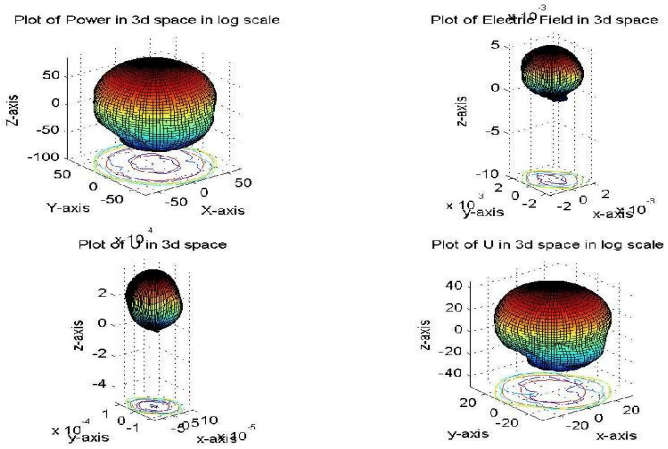

6-j

1250 MHz

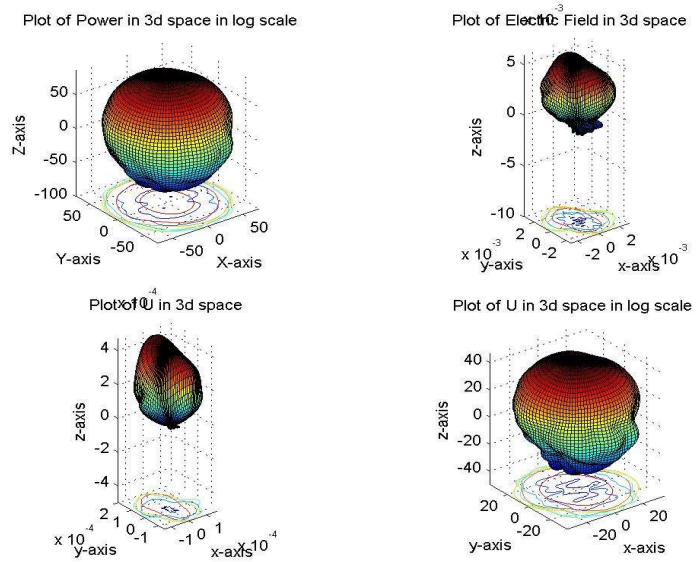

6-k

1500 MHz

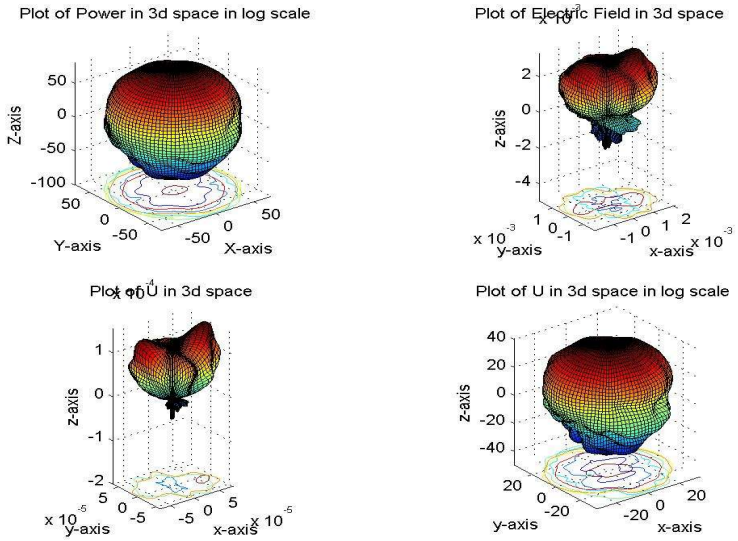

6-l

1750 MHz

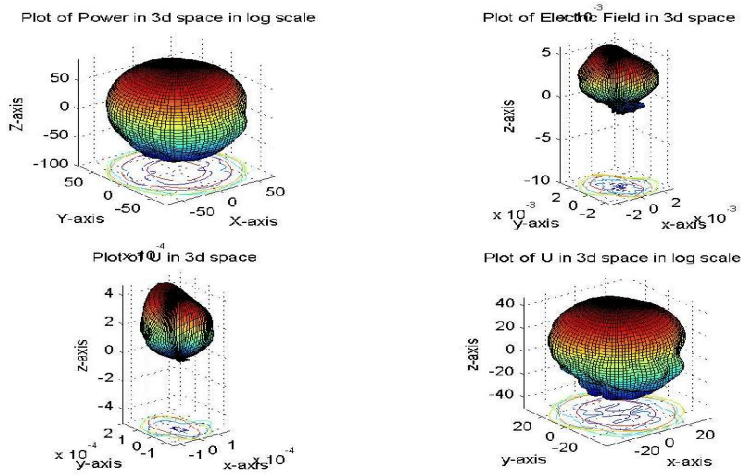

6-m

2000 MHz

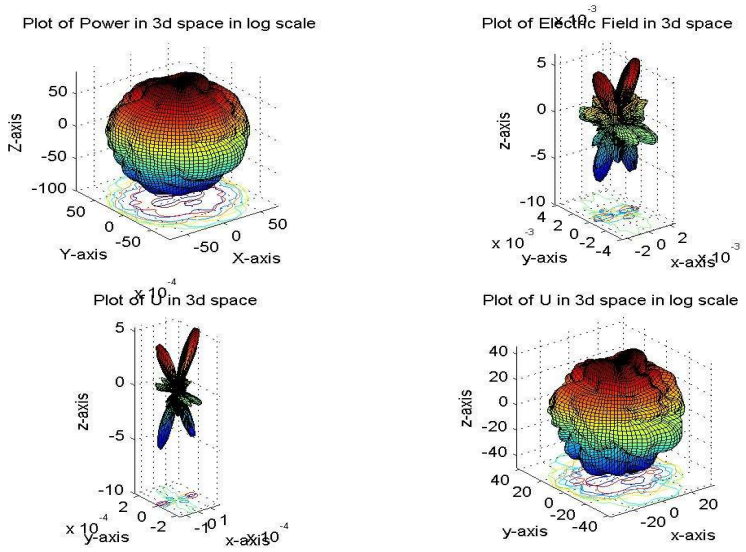

6-n

Fig.6 Three dimensional far-field pattern of power, electric field and radiation intensity

5.2.4 Radiation Intensity Distribution on a Sphere

In the far-field region of the antenna the radiation density has only one radial component. The radiation density decreases according to inverse square law with increasing radius of the observation point. It is therefore more convenient to introduce the radiation intensity, which is the radiation density multiplied by a factor r^2 where r is the magnitude of the radius vector of the observation point with respect to the origin of a three dimensional right handed Cartesian Coordinate system. Therefore the radiation intensity has units of power per unit solid angle and will theoretically be the same for spheres of different

radii surrounding the antenna if the sphere radius is large enough compared to the antenna size and wavelength[4]. In this section the radiation intensity over a large sphere is simulated using MATLAB. In Fig.7 the colour-bar extends from the minimum (black) to the maximum (white) intensity magnitude. The sphere used consists of nearly 500 equal triangles [4].

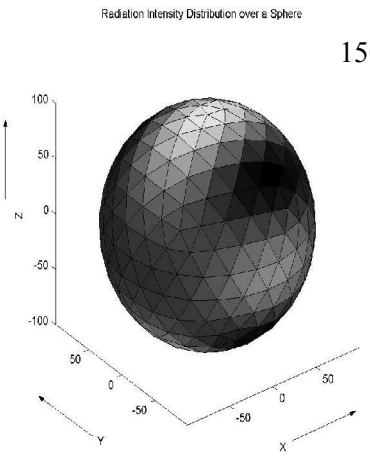

150 MHz

7-a ★

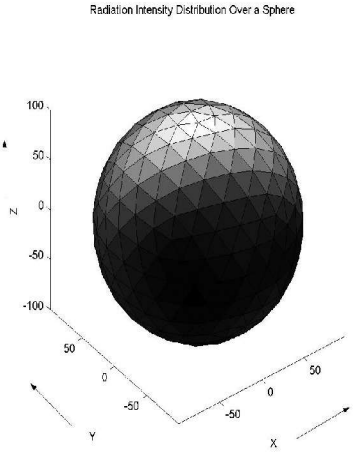

235 MHz

7-b ★

Radiation Intensity Distribution over a Sphere

325 MHz

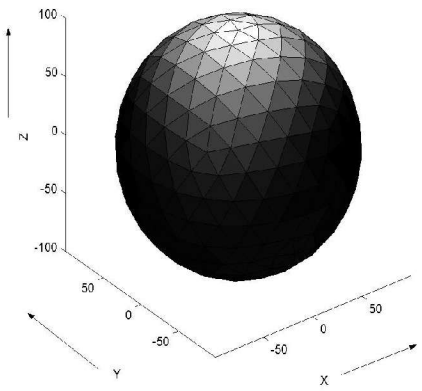

7-c ★

610 MHz

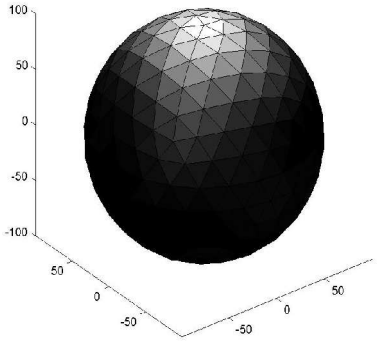

7-d ★

Radiation Intensity Distribution Over a Sphere

1420 MHz

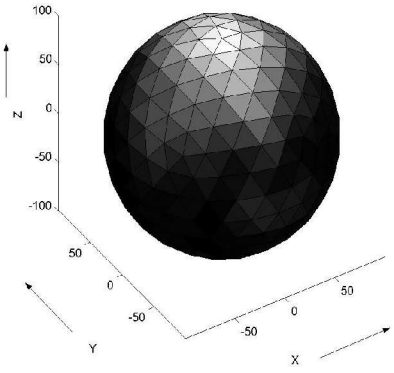

7-e ★

Radiation Intensity Distribution Over a Sphere

1610 MHz

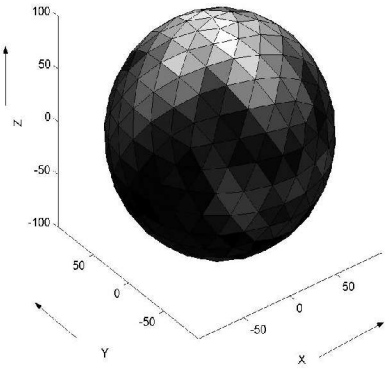

7-f ★

250 MHz

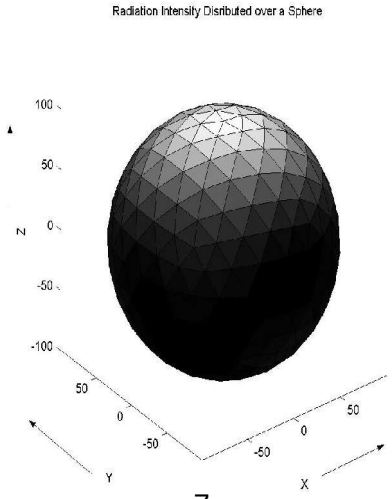

7-g

500 MHz

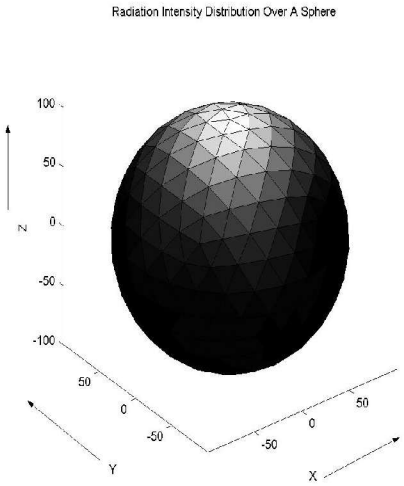

7-h

750 MHz

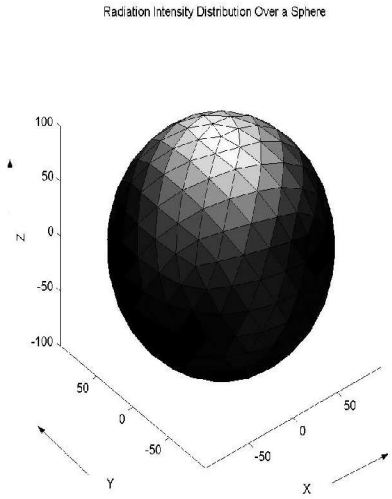

7-i

1000 MHz

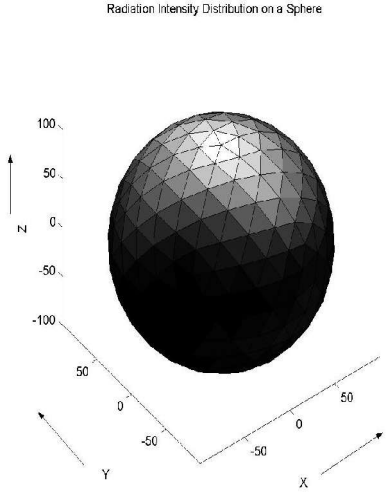

7-j

1250 MHz

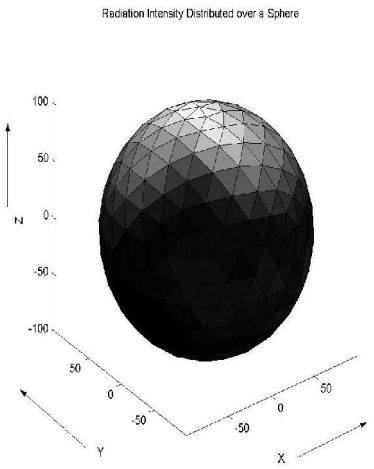

7-k

1500 MHz

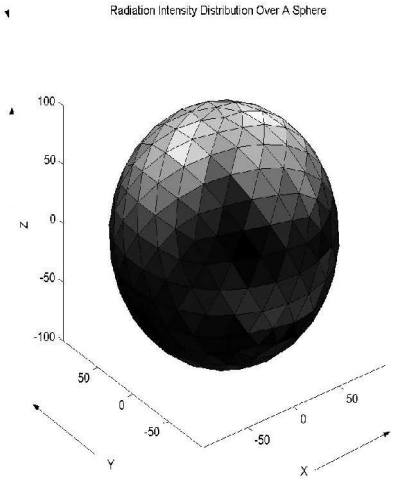

7-l

1750 MHz

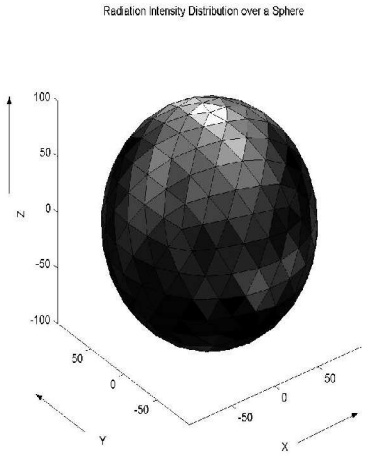

7-m

2000 MHz

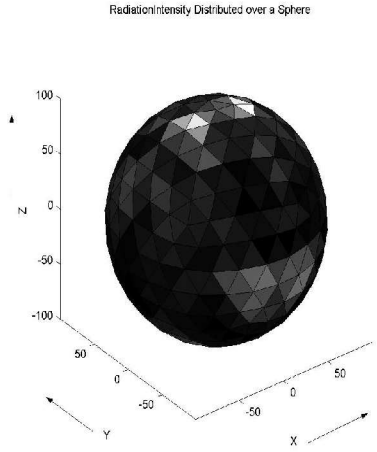

7-n

Fig.7 Radiation intensity distribution on a large sphere

As is seen from Fig.7 the radiation intensity does not show a well defined maximum intensity zone for low frequencies (below 200 MHz,

which is out of the design range). For higher frequencies (1500-2000MHz) a slight deterioration is observed for which investigation is on. For rest of the frequencies (200-1500 MHz) the maximum intensity zone is well defined therefore suggesting that the reflector design in the simulation works well in this band.

N.B (i) Fig.6-a★ to 6-f★ shows the simulation for GMRT frequencies while Fig.6-g to 6-n shows the simulation for a few other general frequencies.

(ii) Fig.7-a★ to 7-f★ shows the simulation for GMRT frequencies while Fig.7-g to 7-n shows the simulation for a few other general frequencies.

Chapter – VI

6.Experiment to Study the Log-Periodic Antenna and Comparison of the Theoretically Obtained Results with the Experimental Ones

6.1 Experimental Setup

The antenna was erected on a wooden stand on the terrace of a tall building (in order to avoid unnecessary reflections) for radiation pattern measurements (Fig. 8).

Fig.8 The radiating and the receiving antennas being mounted on the terrace of two tall buildings.

The incident radiations on the log-periodic antenna used as a receiver

for pattern measurements was made from a half wave dipole (Fig.9) which was mounted on the terrace of an identical building exactly opposite to the building where the log-periodic antenna was placed.

Fig. 9 The radiating dipole used in the experiment

Fig.10 and Fig.11 shows the photographs of the frontal and back portions of the log-periodic antenna, taken while mounted for testing.

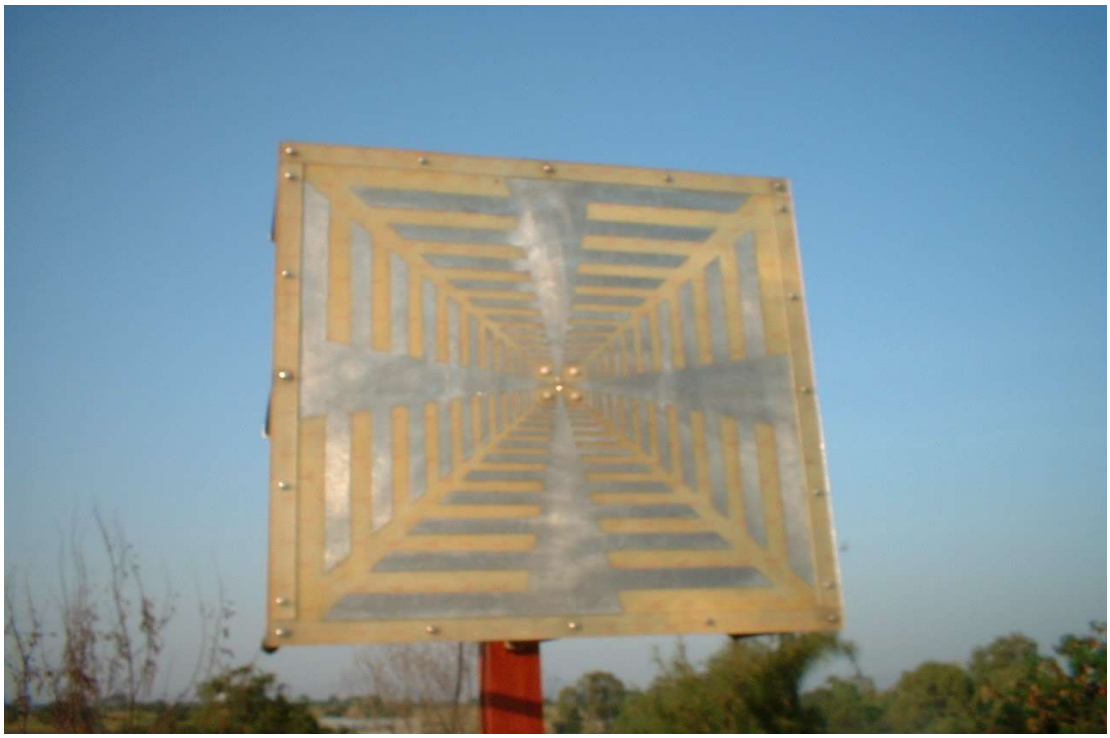

Fig. 10 Front View of the Antenna Mounted for Testing

Fig.11 Back View of the Antenna Mounted for Testing

6.2 Experimental Results and Comparison with Theoretical Simulation

Fig.12-a and b shows the theoretically and experimentally obtained normalized power patterns of the antenna in the E and H planes.

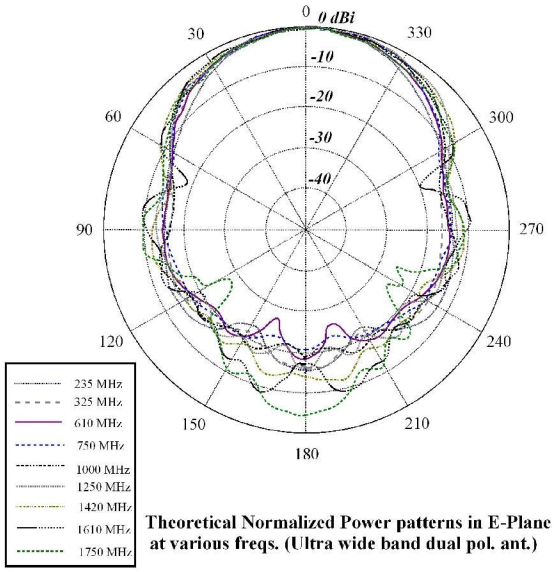

Theoretical Normalized Power patterns in E-Plane at various freqs. (Ultra wide band dual pol. ant.)

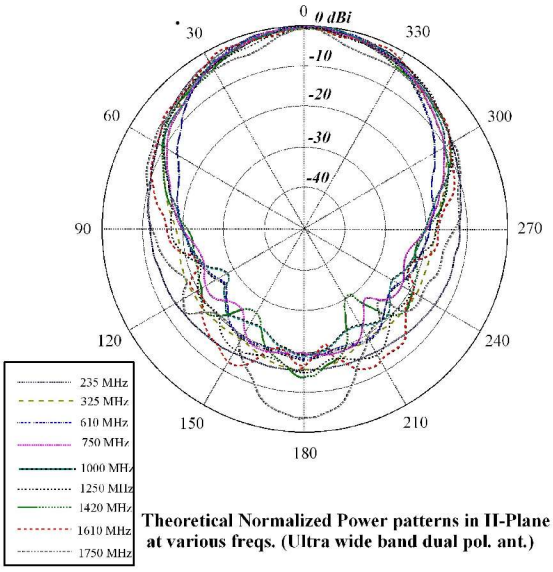

Theoretical Normalized Power patterns in H-Plane at various freqs. (Ultra wide band dual pol. ant.)

12-a Theoretical plots

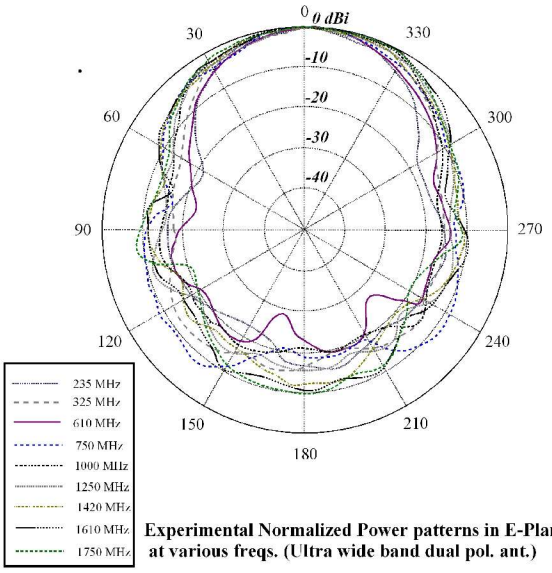

Experimental Normalized Power patterns in E-Plane at various freqs. (Ultra wide band dual pol. ant.)

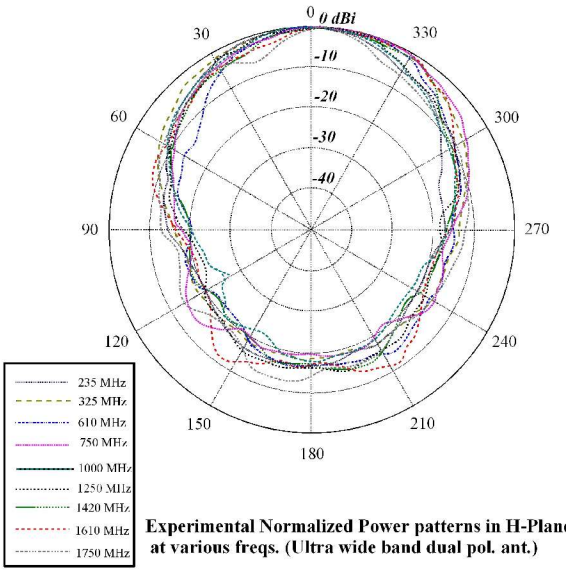

Experimental Normalized Power patterns in H-Plane at various freqs. (Ultra wide band dual pol. ant.)

12-b Experimental plots

From the above plots the variation of gain (in dBi) with changing frequencies is calculated for both the theoretical and the experimentally obtained plots of normalized power patterns, using the Half Power Beam Widths (HPBW) obtained at different frequencies..

The following tables,(Table-A and B) gives the corresponding values.

Table-A : Determination of Theoretical Gain

Frequency(MHz)	HPBW(θ1) in E-Plane (deg)	HPBW(θ2) in H-Plane (deg)	(θ1* θ2) $(deg)^2$	Gain (dBi)
235	45	60	2700	10.46
325	50	52	2600	10.6
610	55	52	2860	10.2
750	52	51	2652	10.5
1000	54	53	2862	10.2
1250	52	33	1716	12.4
1420	60	45	2700	10.46
1610	66	60	3960	8.79
1750	54	20	1080	14.4

Table-B : Determination of Experimental Gain

Frequency(MHz)	HPBW(θ1) in E-Plane (deg)	HPBW(θ2) in H-Plane (deg)	(θ1* θ2) $(deg)^2$	Gain (dBi)
235	44	52	2288	11.17
325	55	80	4400	8.33
610	42	55	2310	11.13
750	44	70	3080	9.88
1000	68	52	3536	9.28
1250	60	55	3300	9.58
1420	58	58	3364	9.50
1610	77	50	3850	8.91
1750	73	24	1752	12.33

The gain was calculated using the following formulas:

$$\text{Linear Gain, } G = (30000)/(\theta 1^* \theta 2)$$

$$\text{Gain (dBi)} = 10 \log_{10} G$$

The following plot (Fig.13) shows the variation of gain with frequency both for simulated and experimentally obtained results.

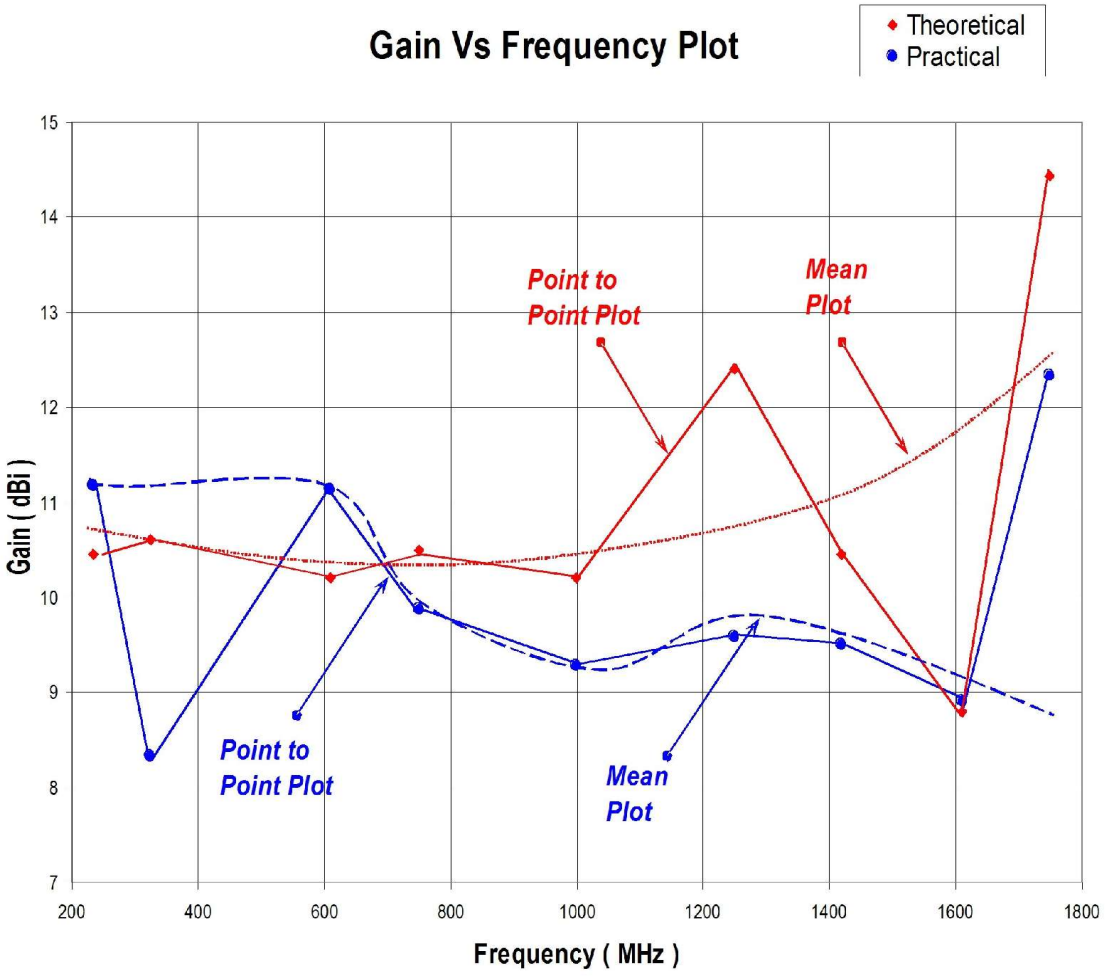

Fig.13 Gain vs frequency plot

From fig.13 (Table-A,Table-B) it is observed that the gain variation is about 6 dB and 4 dB respectively in the theoretical and experimental plots. The theoretical values seem to have more deviation from the mean as compared to the measured values. A fairly well resemblence is observed between theoretical and experimental gain values.

The impedance and reflection coefficient of the antenna were measured using network analyzer which is shown in Fig.14 for a particular polarization. The results of the other polarization antenna are similar to these results.

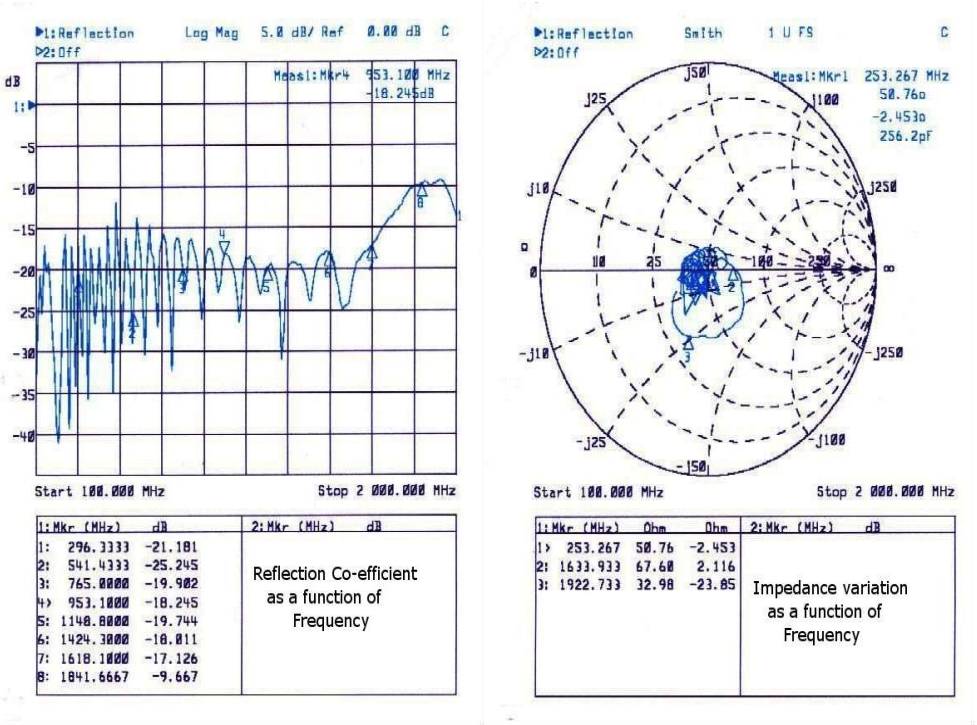

Fig. 14 Reflection coefficient and impedance of the antenna end as a function of frequency

Chapter – VII

7. Conclusions

We have seen in the earlier chapters that the results of the theoretical and experimental results closely match in the designed range of frequencies. The mismatch between the simulated and the experimental plots of the normalized power patterns and radiation intensity needs further investigation. Therefore, it is evident that there is scope of improvement in the theoretical modeling of the antenna-reflector system. The simulation was done mainly for log-periodic antenna. But the simulation algorithms can be used for simulation and analysis of any planar antenna structure [4].

APPENDIX – A

Details of the Antenna Structure Simulation

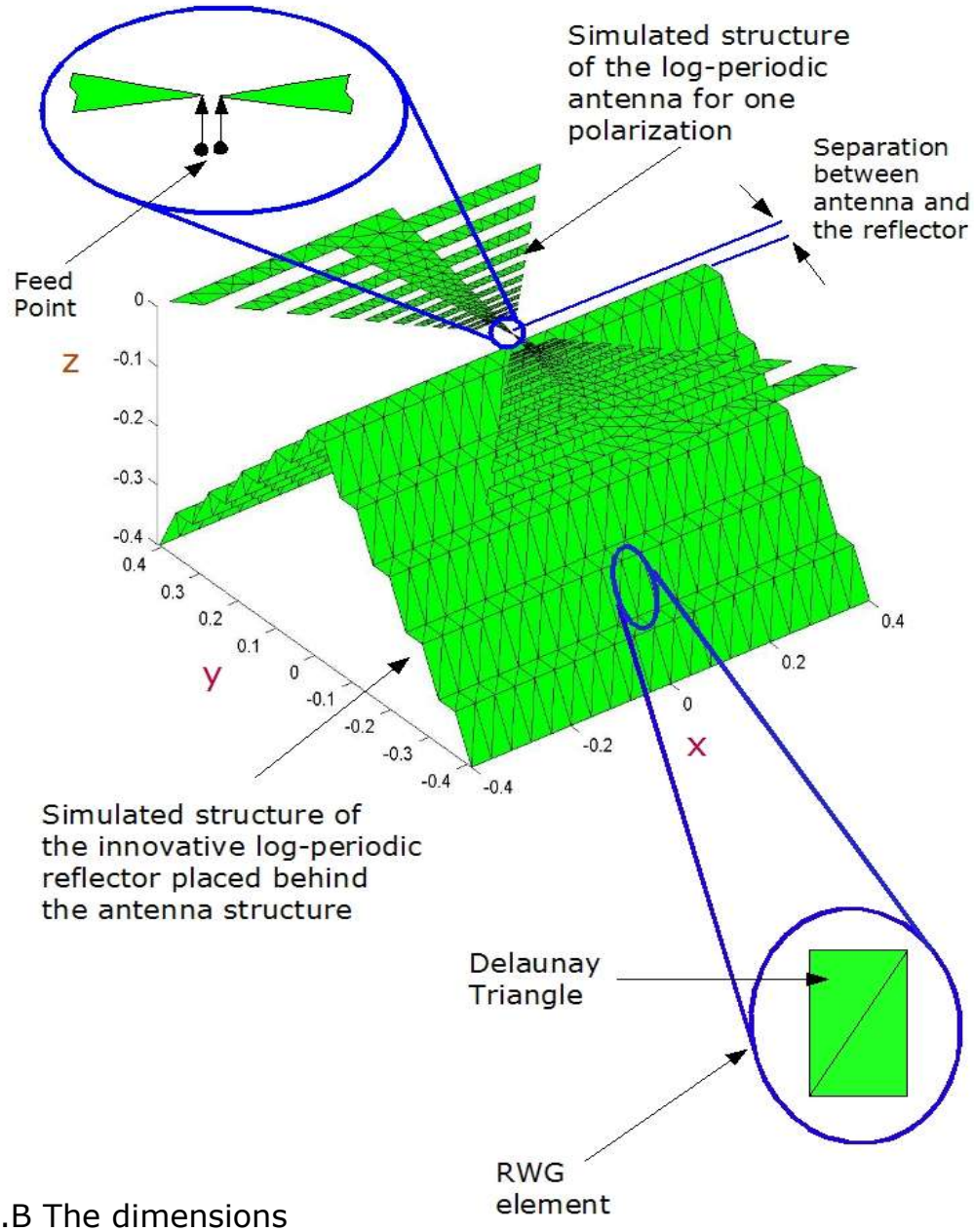

N.B The dimensions are in metres

Fig. A

Fig.A shows the details of the simulated structure of the antenna and the reflector. To model the antenna structure the antenna outline was drawn in the PDE toolbox of MATLAB. Antenna mesh was generated by the mesh generator function of the toolbox which uses Delaunay triangulation to create the mesh on the antenna surface. The mesh was refined several times to obtain the final structure shown in the above figure. A close look at the antenna surface reveals that the triangles on the antenna surface are nearly equilateral triangles[4]. The reflector was designed similarly. The number of steps in the reflector model was less than the actual design because of system limitations. The step sizes were kept equal to simplify the design but actually their size should be proportional to the corresponding antenna elements. There was some small gap between the antenna and the reflector structures as shown in the above figure. The feed was introduced at the small gap between the end points of the two arms of the log-periodic antenna structure as shown in Fig. A.

APPENDIX – B

The 3-D Plotting Algorithm

The basic concept of plotting any variable in 3-d space with MATLAB "Mesh" and "Surface" plotting functions is explained below:

Let, the variable to be plotted in 3-d space be

f= f(r, theta, phi) (1)

where r, theta, phi forms the three dimensional right handed spherical polar coordinate system. Now the rectangular Cartesian coordinates (x, y, z) are related to r, theta, phi by the following relations:

x= r * sin(theta) * cos(phi); (2-a)

y= r * sin(theta) * sin(phi); (2-b)

z = r * cos(theta); (2-c)

where the symbols have their usual meanings. Now as r represents the radius vector of any point in 3-d space with respect to the spherical polar coordinate system, so by replacing r with f(r, theta, phi) in equation (2) and by varying theta from 0 to pi, and phi from 0 to 2*pi, in a nested for loop we get 3 arrays x, y and z in terms of r, theta and phi. Now using the functions mesh(x, y, z) or surf(x, y, z) we generate the 3-d plots.

References

[1] John D.Kraus and Ronald J.Marhefka, " Antennas For All Applications ", 3rd edition, TMH Inc. pg. 386-387.

[2] R.H. DuHamel and D. E. Isbell, " Broadband Logarithmically Periodic Antenna Structures, " *1957 IRE National convention Record,* pt. 1,pg. 119-128.

[3] Constantine A. Balanis, " Antenna Theory", 2nd edition, John Willy and Sons Inc. pg. 552-559.

[4] S. N. Makarov, " Antennas and EM modeling with MATLAB", John Willy and Sons Inc. chapters 1-7.